

# Accepted Manuscript

Wet and dry flexural high cycle fatigue behaviour of fully bioresorbable glass fibre composites: In-situ polymerisation versus laminate stacking

Menghao Chen, Jiawa Lu, Reda M. Felfel, Andrew J. Parsons, Derek J. Irvine, Christopher D. Rudd, Ifty Ahmed



PII: S0266-3538(17)31069-2

DOI: [10.1016/j.compscitech.2017.07.006](https://doi.org/10.1016/j.compscitech.2017.07.006)

Reference: CSTE 6831

To appear in: *Composites Science and Technology*

Received Date: 4 May 2017

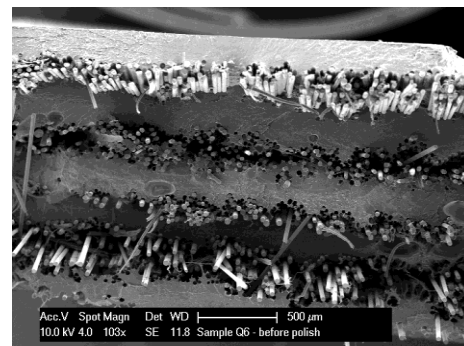
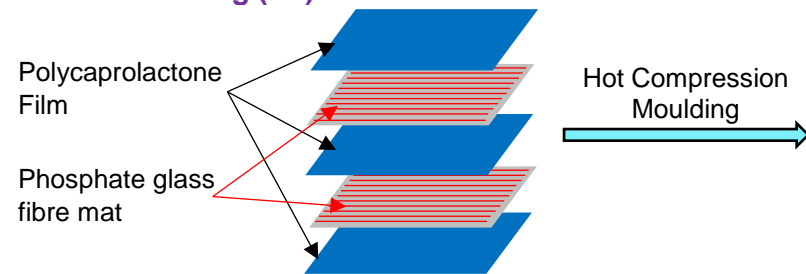
Revised Date: 3 July 2017

Accepted Date: 4 July 2017

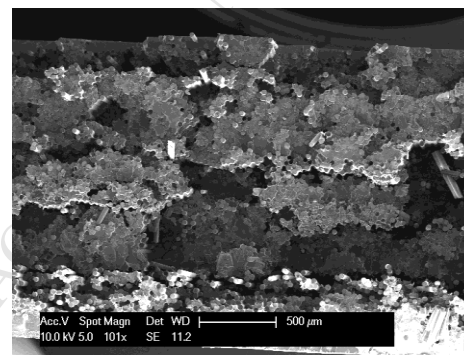
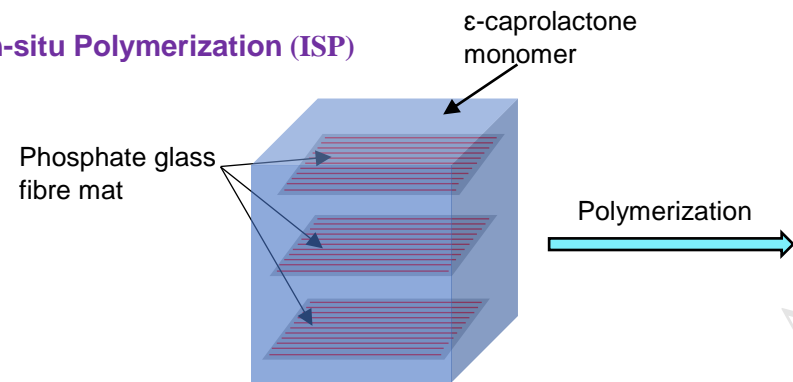
Please cite this article as: Chen M, Lu J, Felfel RM, Parsons AJ, Irvine DJ, Rudd CD, Ahmed I, Wet and dry flexural high cycle fatigue behaviour of fully bioresorbable glass fibre composites: In-situ polymerisation versus laminate stacking, *Composites Science and Technology* (2017), doi: 10.1016/j.compscitech.2017.07.006.

This is a PDF file of an unedited manuscript that has been accepted for publication. As a service to our customers we are providing this early version of the manuscript. The manuscript will undergo copyediting, typesetting, and review of the resulting proof before it is published in its final form. Please note that during the production process errors may be discovered which could affect the content, and all legal disclaimers that apply to the journal pertain.

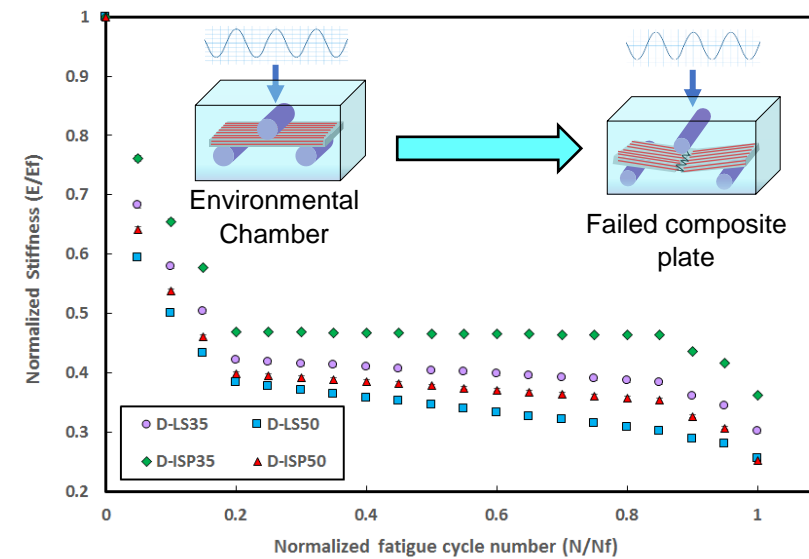
### Laminate Stacking (LS)



### In-situ Polymerization (ISP)



### Flexural Fatigue



# 1 Wet and Dry Flexural High Cycle Fatigue Behaviour of Fully 2 Bioresorbable Glass Fibre Composites: In-situ Polymerisation versus 3 Laminate Stacking

4 Menghao Chen<sup>a</sup>, Jiawa Lu<sup>b\*</sup>, Reda M. Fefel<sup>a, e</sup>, Andrew J. Parsons<sup>c</sup>, Derek J. Irvine<sup>d</sup>, Christopher D. Rudd<sup>b</sup>,  
5 Ifty Ahmed<sup>a\*</sup>

6 <sup>a</sup> Advanced Material Research Group, Faculty of Engineering, University of Nottingham, University Park, Nottingham, UK,  
7 NG7 2RD

8 <sup>b</sup> Department of Mechanical, Materials and Manufacturing Engineering, University of Nottingham Ningbo China, 199  
9 Taikang East Road, Ningbo, 315100, China

10 <sup>c</sup> Composites Research Group, Faculty of Engineering, University of Nottingham, University Park, Nottingham, UK, NG7  
11 2RD

12 <sup>d</sup> Department of Chemical and Environmental Engineering, Faculty of Engineering, University of Nottingham, University  
13 Park, Nottingham, UK, NG7 2RD

14 <sup>e</sup> Physics Department, Faculty of Science, Mansoura University, 35516, Egypt

---

## 15 Abstract

16 Fully bioresorbable phosphate based glass fibre reinforced polycaprolactone (PCL/PGF)  
17 composites are potentially excellent candidates to address current issues experienced with use of  
18 metal implants for hard tissue repair, such as stress shielding effects. It is therefore essential to  
19 investigate these materials under representative loading cases and to understand their fatigue  
20 behaviour (wet and dry) in order to predict their lifetime in service and their likely mechanisms of  
21 failure. This paper investigated the dry and wet flexural fatigue behaviour of PCL/PGF composites  
22 with 35% and 50% fibre volume fraction ( $V_f$ ). Significantly longer flexural fatigue life ( $p < 0.0001$ ) and  
23 superior fatigue damage resistance were observed for In-situ Polymerised (ISP) composites as  
24 compared to the Laminate Stacking (LS) composites in both dry and wet conditions, indicating that  
25 the ISP promoted considerably stronger interfacial bonding than the LS. Immersion in fluid (wet)  
26 during the flexural fatigue tests resulted in significant reduction ( $p < 0.0001$ ) in the composites fatigue  
27 life, earlier onset of fatigue damage and faster damage propagation. Regardless of testing  
28 conditions, increasing fibre content led to shorter fatigue life for the PCL/PGF composites.  
29 Meanwhile, immersion in degradation media caused softening of both LS and ISP composites  
30 during the fatigue tests, which led to a more ductile failure mode. Among all the composites that  
31 were investigated, ISP35 (35%  $V_f$ ) composites maintained at least 50% of their initial stiffness at the  
32 end of fatigue tests in both conditions, which is comparable to the flexural properties of human  
33 cortical bones. Consequently, ISP composites with 35%  $V_f$  maintained at least 50% of its flexural  
34 properties after the fatigue failure, which the mechanical retentions were well matched with the  
35 properties of human cortical bones.

36 **Keywords:** A. Glass fibre, B. Fatigue, C. Damage mechanics, D. Life prediction, In-situ  
37 polymerisation

---

38 *\*Corresponding author at:* Advanced Material Research Group, Faculty of Engineering, University  
39 park,  
40 University of Nottingham, UK, NG7 2RD.

41 Tel: +44 (0)1157484675; +86(0)57488180000 (ext. 8238).

42 Email address: [lfty.ahmed@nottingham.ac.uk](mailto:lfty.ahmed@nottingham.ac.uk); [jiawa.lu@nottingham.edu.cn](mailto:jiawa.lu@nottingham.edu.cn).

## 43 **1. Introduction**

44 In recent decades, fully bioresorbable polymer composites with appropriate biocompatibility  
45 and mechanical properties has provided an exciting opportunity to replace conventional  
46 metal alloy implants, and it has become an active research field because of its excellent  
47 potential in the field of hard tissue repair [1, 2]. Bioresorbable fibre reinforced composites  
48 have been extensively studied utilising different glass fibre compositions, polymer matrices,  
49 fibre architectures and volume fractions. Their mechanical properties range between 200-  
50 700 MPa flexural strength and 15-25 GPa flexural modulus [3-9].

51 Polycaprolactone (PCL)/Phosphate based glass fibre (PGF) composites have been  
52 investigated for developing fully bioresorbable implants [10-13]. PGFs have the ability to  
53 fully dissolve within aqueous media and with adjustable degradation rate [10]. Both PGF  
54 and PCL have also been proven to have good biocompatibility and are considered  
55 favourable materials for biomedical application [3, 4, 14]. However, achieving satisfactory  
56 fibre-matrix interface adhesion and retention, thus appropriate composite mechanical  
57 properties for bone fracture fixation has been the main restriction [3, 5, 6, 15]. Studies have  
58 recognised the weak fibre-matrix interface is mainly due to poor fibre impregnation, which  
59 can result from the high viscosity of the melted matrix involved in traditional laminate  
60 stacking (LS) and hot press moulding [5, 13, 16]. To promote a more durable fibre-matrix  
61 interface, a novel in-situ polymerisation (ISP) technique has been developed to  
62 manufacture PCL/PGF composites in the group [16, 17]. There is solid evidence that  
63 suggested that ISP can promote a significantly stronger and more robust fibre-matrix  
64 interface than LS, with accordingly higher mechanical properties and prolonged retention of  
65 properties during degradation [13, 16-19]. Furthermore, the biocompatibility of the ISP PCL  
66 was investigated via Alamar blue assay using osteoblasts derived from human craniofacial  
67 bone cells. The results indicated that ISP PCL was highly biocompatible, and the residual  
68 monomer (Measured by Nuclear Magnetic Resonance) did not significantly affect the  
69 biocompatibility of the composites [19].

70 The flexural fatigue properties are of vital importance for bone fracture fixation implant  
71 applications. The main application for the PCL/PGF composites is as bone fracture fixation  
72 devices and has initially focused on bone repair plates, for which the primary loading would

73 be in flexure mode and as such was the focus for this study [20-22]. Typical time required  
74 for bone fracture healing is 8-12 weeks, where the composites will be subject to dynamic  
75 body fluid and constant body temperature [20, 21, 23]. The majority of previous studies on  
76 fibre reinforced composites have indicated that elevated humidity and temperature  
77 generally severely shortened their fatigue life [24-27]. Composites fatigue behaviour is a  
78 complex phenomenon, which is generally studied by crack initiation, crack multiplication  
79 and final failure [28-30]. Damage mechanisms in flexural fatigue of fibre reinforced  
80 composites, in general, involve matrix cracking, fibre breakage and interface failure [31, 32].  
81 The diffusion and growth of composites fatigue damage resulting from crack bridging and/or  
82 fibre/matrix de-bonding is governed by the behaviour of fibre/matrix interaction [31, 33-35].  
83 The diffuse damage growth often results in a gradual decrease of the composite's stiffness  
84 with growing loading cycles, which is coupled with a significant increase in the composite's  
85 material damping [36]. The damping mechanisms of fibre reinforced composites are  
86 governed mainly by thermo-elastic damping, Coulomb friction damping of the fibre-matrix  
87 interface, energy dissipation at cracking/delamination and the viscoelastic nature of the  
88 fibre and matrix material [37, 38]. Both stiffness evolution and material damping are often  
89 used as sensitive indicators to study the damage mechanisms of composites [39-43]. Shah  
90 [44] systematically studied the stiffness evolution of plant fibre reinforced composites  
91 subjected to tensile fatigue loading, where stiffness profiles were used to investigate  
92 composite damage initiation and accumulation. Gassan [38] investigated the fatigue  
93 behaviour of natural fibre (flax and jute) reinforced polymer composites using specific  
94 damping capacity (SDC) as a sensitive indicator for monitoring the behaviour of material  
95 damage.

96 Despite the extensive studies on the mechanical performance of implant biomaterials, their  
97 time-dependent fatigue behaviour is still poorly understood. Fatigue properties are of  
98 paramount importance for their intended application where components are subjected to  
99 various loading and environmental parameters, which vary with time over the period of  
100 service. The target properties of the composites were within the properties reported for  
101 human cortical bone, i.e. 5-23 GPa and 35-280 MPa for flexural modulus and strength  
102 respectively [45]. There are several studies of fatigue behaviour for metal alloy and bone  
103 cement composite implant biomaterials, which well pointed out the significance of fatigue  
104 strength and life in the design and use of implant devices [46]. However, up to the best of

105 the authors knowledge, cyclic fatigue response of the fully resorbable composites has not  
106 been explored yet.

107 In this study, PCL/PGF composites with  $V_f$  of 35% and 50% were produced using LS and  
108 ISP techniques. Environmental flexural fatigue tests were performed on these composites  
109 in both dry conditions at ambient temperature and in wet conditions immersed in phosphate  
110 buffered saline (PBS) solution at 37 °C. The wet conditions were intended to mimic the  
111 physiological nature of the human body. Both stiffness reduction and SDC were used as  
112 sensitive indicators to monitor the damage initiation of the composites during cyclic loading.  
113 The influences of solution immersion, fibre content and fibre-matrix adhesion on the  
114 performance of the PCL/PGF composites were investigated by comparing their fatigue  
115 behaviour.

## 116 **2. Materials and Methods**

### 117 **2.1. Materials**

118 Monomer  $\epsilon$ -caprolactone (97% purity),  $\text{Sn}(\text{Oct})_2$  (92.5%-100% purity) and benzyl alcohol  
119 (99.8% purity) were obtained from Sigma Aldrich (UK). PCL pellets were also obtained from  
120 Sigma Aldrich (UK) and with a molecular weight ( $M_w$ ) of ~65,000 g/mol.

### 121 **2.2. Phosphate based glass and glass fibre**

122 Phosphate based salts were used to produce fully bioresorbable phosphate glass (Sigma  
123 Aldrich, see Table 1 for detailed glass formulation). A specific salt mixing and melting  
124 scheme was used to produce the phosphate based glass. PGFs were made using in-house  
125 designed melt-draw equipment comprised of a furnace (Lenton Furnaces, UK) with a Pt/10%  
126 Rh crucible (Johnson Matthey, UK). Phosphate glass and glass fibre mats were stored in a  
127 desiccator to minimise any potential moisture adsorption. The fibre mats were then dried in  
128 a 50 °C vacuum oven for 24 hours before use. For the detailed manufacturing process and  
129 parameters, please refer to the authors' previous paper [13].

### 130 **2.3. PCL/PGF composites**

131 Composites with 35% and 50% fibre volume fraction ( $V_f$ ) were manufactured via both ISP  
132 and LS. Respective composite codes and specifications are listed in Table 2.

#### 133 **2.3.1. Laminate stacking (LS) technique**

134 PCL thin films were manufactured and PGF mats were stacked with the thin films to hot  
135 compress into composites. Detailed processes can be found in the authors' previous paper

136 [13]. The composite plate was made into test specimens with dimensions of 40mm × 15mm  
137 × 2mm by a band saw.

### 138 2.3.2. In-situ polymerisation (ISP) technique

139 PTFE moulds with two injection ports were designed and used to produce PCL/PGF  
140 composites in one single step.  $\epsilon$ -caprolactone was degassed via a freeze-thaw-pump  
141 process to minimise the moisture content within the solution. Reaction mixture of  $\epsilon$ -  
142 caprolactone with pre-determined amount of catalyst and initiator was injected into the  
143 mould cavity and PCL was polymerised directly around the PGF mats. Ring opening  
144 polymerisation was utilised for PCL polymerisation during the ISP process. Detailed mould  
145 design and explanation of the in-situ process can be found in author's previous paper [13].  
146 Resulting composite plates were cut into dimensions of 40mm × 15mm × 2mm using a  
147 band saw.

## 148 2.4. Flexural testing

### 149 2.4.1. Monotonic loading

150 Monotonic 3-point bending tests were conducted on a Bose ElectroForce® Series II 3330  
151 testing machine. The testing machine is equipped with an environmental chamber, which  
152 enables tests within liquid at various temperatures (See Figure 1). BS EN ISO 14125:1998  
153 was followed for all tests. Sample dimensions of 40mm × 15mm × 2mm, a cross-head  
154 speed of 1 mm/min and a 3 kN load cell was used. Tests were carried out in triplicate (n=3).  
155 Composites were tested in two environments: at ambient temperature and in dry conditions  
156 (Dry Environment) and at 37 °C submerged in PBS solution (Wet Environment). The  
157 samples were immersed in PBS heated to 37°C for 5 minutes to allow PBS and testing  
158 temperature equilibrate prior to testing. Displacement/deflection loads were measured via  
159 the testing machine, for which the stress and strain were calculated according to the  
160 equations stated in BS EN ISO 14125:1998 as below:

$$\sigma_f = \frac{3FL}{2bh^2} \quad (1)$$

$$\varepsilon = \frac{6sh}{L^2} \quad (2)$$

161 Where  $\varepsilon$  is the strain,  $\sigma_f$  is the stress, s is the measured displacement, F is the measured  
162 load, b is the sample width, h is the sample thickness and L is the sample span length.

### 2.4.2. Cyclic loading

Flexural fatigue tests (Load-controlled) were conducted on a Bose ElectroForce® Series II 3330 testing machine. Figure 2 presents a sample load waveform (5 Hz) applied during the fatigue tests (Specific fatigue terms and R-values defined). In accordance with BS ISO 13003:2003, at least 5 samples were examined to failure at six stress levels for the determination of the composites' stress-lifetime diagrams. All the composites were tested in 3-point bending mode (Bending-bending condition) with a stress ratio of  $R = 0.1$ . Calculations for flexural stress and strain were performed according to BS EN ISO 14125:1998. Shear effects were taken into consideration for the stress and strain calculations since the deflection of the specimens during the fatigue tests was relatively large.

When the measured deflection was less than 10% of the sample span length, the flexural stress and strain were calculated via equation 1 and 2. When the measured deflection was larger than 10% of the sample span length, equation 3 and 4 below were used:

$$\sigma_f = \frac{3FL}{2bh^2} \left\{ 1 + 6 \left( \frac{s}{L} \right)^2 - 3 \left( \frac{sh}{L^2} \right) \right\} \quad (3)$$

$$\varepsilon = \frac{h}{L} \left\{ 6 \frac{s}{L} - 24.37 \left( \frac{s}{L} \right)^3 + 62.17 \left( \frac{s}{L} \right)^5 \right\} \quad (4)$$

Where  $\sigma_f$  is the flexural stress,  $\varepsilon$  is the strain,  $s$  is the beam mid-point deflection,  $F$  is the load,  $L$  is the span length,  $h$  is the thickness of the specimen and  $b$  is the width of the specimen.

Fatigue tests were performed in both dry and wet testing conditions. Testing the dry composites at room temperature was known as the dry testing condition and wet testing condition referred to testing the submersed composites in PBS solution and at 37 °C. A KTJ TA318 thermometer & hygrometer was used to measure the temperature and relative humidity of the dry testing conditions, which were in the range of 15 °C - 22 °C and 44% - 53% respectively. Stress levels for all fatigue tests were 80%, 70%, 60%, 50%, 40% and 30% of the corresponding Ultimate Flexural Strength (UFS) for each type of composite.

Figure 3 showed an example of the stress strain variation of a composite sample during fatigue testing. The loading cycles plotted were selected as 1 out of every 1000 loading cycles and each loop in Figure 3 represents a full loading cycle. Flexural stiffness of the



190 composite can be calculated from each loading cycle and the variation in their strain can  
191 also be recorded.

## 192 **2.5. Fatigue data analysis**

### 193 **2.5.1. Stress-Life (S-N) diagram**

194 As illustrated in Figure 4, a typical Wohler Stress-Life (S-N) diagram [31] is plotted as stress  
195 amplitude ( $\sigma_a$ ) against number of fatigue cycles to failure ( $N_f$ ) (See Figure 4). S-N curves  
196 are normally fitted with a power regression relationship, named Basquin's equation  
197 (Equation 5) [31].

$$198 \quad \sigma = aN_f^b \quad (5)$$

199 Where  $\sigma$  is a generic term describing cyclic stress (in this case  $\sigma_a$ , see Figure 2),  $N_f$  is a  
200 generic term describing fatigue life (in this case cycles to failure) and  $a$  &  $b$  are material  
201 constants specific to each material. The constant ' $b$ ' is used as an important parameter in  
202 this study to indicate the sensitivity of the fatigue life to the applied stress. The value of ' $b$ '  
203 represents the slope of the SN curve, thus the decline rate of fatigue strength.

### 204 **2.5.2. Specific Damping Capacity (SDC)**

205 To study and monitor the progress of composite damage during the fatigue tests, SDC was  
206 used as a sensitive indicator throughout this study. As damage progresses, the composite  
207 specimens show reductions in strength and modulus as well as a significant increase in  
208 their own damping [38, 47]. Changes in material damping capacity can be observed as a  
209 function of the stress levels during the fatigue tests [48]. An example is illustrated  
210 graphically in Figure 5.

211 In this paper, SDC was measured to determine the critical applied stress (CAS) for damage  
212 initiation of both the LS and ISP composites within 104 fatigue loading cycles. This cycle  
213 number (104) was chosen since it is the general divider between low and high cycle fatigue  
214 behaviour [31]. A similar method was used by Gassan et. al to measure the CAS values for  
215 studying fatigue damage behaviour of fibre reinforced composites [38]. The CAS is an  
216 important factor for load bearing applications, such as fracture fixation devices, as it sets  
217 the limitations of the composite loading capacity under cyclic loading conditions. Any  
218 applied cyclic stress higher than the measured CAS would imply material damage within  
219 104 loading cycles.

220 In order to obtain SDC values for the composites, a fatigue test is performed using constant  
221 values of stress level, R and frequency (R=0.1, 5 Hz) for a defined number of load cycles  
222 ( $10^4$  cycles in this case). Fresh LS and ISP composites (non-degraded) were used for the  
223 SDC study. Subsequently, the fatigue test was repeated for the same number of load  
224 cycles at a higher stress levels. This continued until the specimen failed. A minimum of n=5  
225 samples were tested for each category of composites. Tests were carried out in both dry  
226 and wet testing conditions, using the stress levels specified in 2.4.2. The value of SDC was  
227 then calculated using Equation 6 [38, 49]:

$$228 \quad SFDC = \Delta U/U = (U_I - U)/U \quad (6)$$

229 Where  $U$  is the maximum strain energy stored by the specimen during one loading cycle,  
230  $\Delta U$  is the energy dissipated only by the specimen during one loading cycle (such as friction  
231 damping caused by de-bonding, crack and delamination) and  $U_I$  is the input energy from  
232 the system to the specimen during one cycle. Strain energy was calculated by integrating  
233 the area within the loading loop (See Figure 3 shaded area) at a defined number of load  
234 cycles. Input energy was calculated by integrating the loading and displacement history  
235 from the testing machine.

## 236 **2.6. Scanning Electron Microscopy (SEM)**

237 SEM was performed on freeze-fractured specimens after testing to study the matrix/fibre  
238 interface and failure mode. 10 keV Voltage was applied with secondary electron mode.  
239 Platinum was sputter-coated on all composites samples before imaging.

## 240 **2.7. Burn off test**

241 Actual fibre volume fractions of both LS and ISP composites were determined by burn off  
242 tests. BS EN ISO 2782-10 was applied for all burn off tests. Table 3 reports all results (n=5).

## 243 **2.8. Statistical analysis**

244 Data were presented in tables and figures as mean  $\pm$  standard deviation. Microsoft Excel  
245 was used to analyse the data and a student's unpaired t-test was performed to determine  
246 the statistical significance as below: statistically insignificant ( $p>0.05$ ), statistically significant  
247 ( $p<0.05$ ), very statistically significant ( $p<0.01$ ) and extremely statistically significant  
248 ( $p<0.0001$ ).

### 3. Results

#### 3.1. Composites fibre content and quasi-static flexural properties

Table 3 below shows the fibre volume fractions, quasi-static flexural strength and modulus for all the LS and ISP composites tested in both dry and wet testing conditions.

#### 3.2. S-N diagrams

Figure 6 shows the variation of the fatigue life for each of the composites tested versus increasing stress levels in both dry and wet testing conditions. A good fit can be seen from the Basquin's equation (Equation 5) to the experimental data, with  $R^2$ -value  $> 0.9$  for all regressions. Table 4 shows the values of 'b' obtained from curve fitting the experimental fatigue data using the Basquin's equation.

A gradual decrease in fatigue life with increasing stress levels was observed for all composites, as expected. It was also observed that the 35%  $V_f$  composites showed a significantly longer fatigue life ( $p < 0.01$ ) than their equivalent 50%  $V_f$  composites (See Figures 6a and 6b). In dry conditions at the same stress level, D-LS35 and D-ISP35 showed ~29% and ~34% longer fatigue life respectively, when compared to D-LS50 and D-ISP50. However, in wet conditions, the W-LS35 and W-ISP35 showed ~20% and ~23% longer fatigue life than W-LS50 and W-ISP50.

Comparing Figures 6a and 6b, immersion in PBS solution at 37 °C substantially decreased the fatigue life for both ISP and LS composites. At the same stress level, the dry D-LS35 and D-LS50 samples showed approximately 10 times longer fatigue life than the wet W-LS35 and W-LS50 samples respectively. For example, D-LS35 exhibited ~3 million cycles to failure at 30% UFS stress level, whilst the wet W-LS35 samples lasted only ~50,000 cycles. Similarly, D-ISP35 and D-ISP50 exhibited approximately 9 times longer fatigue life than W-ISP35 and W-ISP50 (i.e. ~4 million and ~230,000 cycles to failure for D-ISP35 and W-ISP35 respectively at 30% UFS stress level).

Regardless of the testing conditions, the ISP composites demonstrated a substantially longer fatigue life ( $p < 0.0001$ ) than the LS composites of equivalent  $V_f$ . When tested in a dry environment and at the same stress level, the D-ISP35 and D-ISP50 showed ~25% and ~19% longer fatigue life than D-LS35 and D-LS50 respectively (See Figure 6a). Similarly, in wet conditions, the W-ISP35 and W-ISP50 exhibited ~85% and ~74% longer fatigue life than W-LS35 and W-LS50 (See Figure 6b).

### 280 3.3. Failure strain variation

281 Figures 7a and 7b show the variation of failure strain versus the stress levels tested. The  
282 vertical dotted line represents the threshold stress level at which the failure strains increase  
283 significantly ( $p < 0.01$ ). The LS composites showed significantly lower failure strain profiles  
284 ( $p < 0.01$ ) than ISP composites in both dry and wet conditions. By comparing ISP and LS  
285 composites (identical  $V_f$ ) in dry conditions (See Figure 7a), no significant difference ( $p > 0.01$ )  
286 was found in the increase rate of failure strain with increasing stress levels. However, in wet  
287 conditions, the W-ISP50 samples showed a significantly faster increase rates of failure  
288 strain than the W-LS50 (See Figure 7b).

289 When tested in the same conditions, both LS and ISP composites with 50%  $V_f$  showed  
290 significantly lower ( $p < 0.01$ ) failure strain values in comparison to composites with 35%  $V_f$   
291 for all stress levels. Figures 7a and 7b, also showed that the LS and ISP composites had  
292 significantly higher failure strain value profiles ( $p < 0.01$ ) in dry conditions compared to wet  
293 conditions. When tested dry, the failure strain value of D-LS35 and D-LS50 started to  
294 increase at 50% UFS stress level, while 60% UFS stress level (See the dotted vertical line  
295 in Figure 7) was observed for D-ISP35 and D-ISP50. However, in wet conditions, the  
296 increase was observed from 40% UFS stress level for all LS and ISP composites.

### 297 3.4. Stiffness evolution

298 The stiffness evolution profiles are presented in Figures 8a and 8b below, which show  
299 gradual decline of the composites' stiffness during their fatigue life at a specific stress level  
300 (40% of UFS). The initial stiffness  $E_f$  was determined from the first loading cycle and the  
301 residual stiffness,  $E$  at  $n$  cycles of the loading loop (See Figure 3).

302 Substantial differences were observed when comparing the stiffness at failure, following the  
303 trend of D-ISP35 > D-LS35 > D-ISP50 > D-LS50 > W-ISP35 > W-LS35 > W-ISP50 > W-  
304 LS50 for all stress levels investigated. For example, at 40% UFS stress level, D-ISP35  
305 exhibited ~60% stiffness at failure whilst W-LS50 demonstrated ~30% residual stiffness at  
306 failure.

307 Comparing Figures 8a and 8b, the ISP composites revealed significantly higher stiffness  
308 profiles ( $p < 0.01$ ) than the LS composites through their entire fatigue life. Moreover,  
309 composites with 35%  $V_f$  showed considerably higher stiffness profiles throughout the  
310 fatigue life and slower stiffness reduction rates than composites with 50%  $V_f$  in the same  
311 testing condition. The change from dry to wet condition resulted in significantly lower

312 stiffness profiles ( $p < 0.01$ ) and faster stiffness reduction rates ( $p < 0.01$ ) for all the LS and ISP  
313 composites.

314 According to Figure 8a, there was a distinct increase in stiffness at the beginning of the  
315 composites fatigue life in dry conditions. Meanwhile, in wet conditions, the stiffness profiles  
316 showed a gradual decline from the beginning of the fatigue life (See Figure 8b). Moreover,  
317 in dry testing conditions, it was found that with tests performed at stress levels over 50% of  
318 respective UFS, no initial increase was seen and a gradual decline from the beginning of  
319 the fatigue tests was also observed (See inset graph of Figure 8a).

### 320 **3.5. Specific Damping Capacity (SDC)**

321 Figure 9 shows the variation of SDC versus increasing maximum applied stress for both LS  
322 and ISP composites tested in dry and wet conditions. The critical applied stress (CAS) for  
323 damage initiation of the composites was estimated as the stress where SDC starts to  
324 increase significantly ( $p < 0.01$ ) and they are indicated by arrows in Figure 9 [38].

325 Table 5 showed the CAS values for all composites tested. Regardless of the testing  
326 environment, significantly higher CAS ( $p < 0.01$ ) values can be seen for ISP composites than  
327 for the LS composites. Moreover, with the same manufacturing method and in dry  
328 conditions, composites with 35%  $V_f$  showed significant higher CAS ( $p < 0.01$ ) than  
329 composites with 50%  $V_f$ . Meanwhile, 50% composites showed lower CAS values than 35%  
330 composites in wet conditions. In dry conditions (Figure 9a), only D-LS50 had significantly  
331 higher SDC profile ( $p < 0.01$ ) against increasing applied stress than other composites.  
332 However, in wet conditions (Figure 9b), both W-LS35 and W-LS50 showed distinctly higher  
333 SDC profiles ( $p < 0.01$ ) than W-ISP35 and W-ISP50 respectively. By comparing Figures 9a  
334 and 9b, the CAS values for W-LS35, W-LS50, W-ISP35 and W-ISP50 were ~30%, ~41%,  
335 ~41% and ~49% lower than D-LS35, D-LS50, D-ISP35 and D-ISP50 respectively.

### 336 **3.6. SEM Analysis**

337 Figure 10 compared the cross sections of the composite fracture surfaces between LS and  
338 ISP composites tested within both dry and wet conditions. Clear polymer rich zones and  
339 fibre pull-outs were seen from the SEM micrographs of LS35 and LS50 (Figure 10a, 10e  
340 and Figure 10c, 10g). Meanwhile, clean fibre fractures with no visible polymer rich zones  
341 were observed from the SEM micrographs of ISP35 and ISP50 (Figure 10b, 10f and Figure  
342 10d, 10h).

343 Figure 11 displayed the typical fatigue failure modes of the LS and ISP composites tests in  
344 both dry and wet conditions. In dry conditions, LS composites showed compressive  
345 delamination and interlaminar shear fracture failure modes (Figure 11a and 10b), whilst ISP  
346 composites showed clean centre fracture (Figure 11c). In wet conditions, the LS  
347 composites showed softening behaviour with interlaminar shear fracture failure mode  
348 (Figure 11d and 11e), whilst the ISP composites showed fibre sliding behaviour with centre  
349 fracture failure mode (Figure 11f).

#### 350 **4. Discussions**

351 This study investigated the cyclic flexural fatigue performance of PCL/PGF composites ( $V_f$   
352 of 35% and 50%) produced via LS and ISP processes. Environmental conditions were  
353 evaluated by performing tests in dry (room temperature) and in wet conditions (immersed in  
354 PBS at 37 °C). Fatigue behaviour of the composites was characterised via the classic S-N  
355 diagrams, stiffness degradation profiles and specific damping capacity (SDC).

356 Table 3 summarises the quasi-static flexural properties of the LS and ISP composites in  
357 both dry and wet conditions. Testing the samples in wet conditions revealed significant  
358 reductions in both the stiffness and strength of the composites, compared to the dry tested  
359 samples. Several studies have been conducted on similar PGF composites, which  
360 investigated quasi-static mechanical properties in dry and wet conditions. They also  
361 reported a distinct decrease in flexural strength and modulus for samples tested in quasi-  
362 static wet conditions, and suggested this was due to media attack disrupting the fibre matrix  
363 interface and plasticisation [3, 5, 13, 50]. However, the ISP composites revealed  
364 considerably higher flexural properties compared to the LS composites in both dry and wet  
365 conditions. A previous study [13] revealed that a stronger and more robust fibre/matrix  
366 interface was promoted by the ISP process as compared to LS, which inhibited PBS media  
367 attack and revealed a significant increase in the composite flexural properties (by ~45%).

368 Factors influencing the fatigue behaviour were characterised taking into consideration three  
369 key factors as discussed below.

##### 370 **4.1. Influence of fibre-matrix interface**

371 The S-N diagrams produced revealed the fatigue life profiles with increasing testing stress  
372 for all the LS and ISP composites tested (See Figure 6). It was immediately apparent that  
373 the ISP composites demonstrated a significantly longer fatigue life ( $p < 0.0001$ ) than the LS  
374 composites at each stress level in both dry and wet conditions. This major increase in

375 fatigue life was attributed to sturdier interfacial bonding achieved by the ISP manufacturing  
376 process. De-bonding of the fibre/matrix interface (especially ductile matrices, such as PCL)  
377 is widely considered to be the main governing factor of crack propagation, which can lead  
378 to fatigue failure of fibre reinforced composites [31, 51, 52]. Weak interfacial properties can  
379 allow de-bonding and friction sliding between fibre and matrix to occur readily upon crack  
380 propagation, which can lead to matrix cracks (In this case delamination, see Figures 11a  
381 and 11b) without major fibre fractures [33, 53]. Conversely, a stronger fibre/matrix interface  
382 could inhibit interfacial sliding and lead to direct fibre fractures along with cracks in the  
383 matrix, without inducing significant de-bonding of the fibre/matrix interface (see Figure 11c)  
384 [33, 51, 53]. This difference in behaviour was apparent when comparing ISP and LS  
385 composites, as illustrated by the failure cross sections in Figure 10. LS composites showed  
386 significant fibre pull-out and ISP composites had clear fibre fractures, which demonstrated  
387 that a stronger fibre/matrix interface for the ISP samples had been achieved. Several  
388 studies have investigated the effects of the fibre/matrix interface on the fatigue behaviour of  
389 glass or carbon fibre reinforced composites. The studies applied coupling agents on fibre  
390 surfaces to promote stronger interfacial bonding with the polymer matrices and  
391 consequently significantly longer fatigue lives (ranging from 5% - 20%) were achieved [38,  
392 47, 52, 54]. It should be noted that improvements in fibre/matrix interfacial properties in this  
393 study were achieved via the ISP manufacturing process alone, and without the use of  
394 coupling or sizing agents. This suggests that the ISP process can promote strong interfacial  
395 bonding of fibre reinforced composites and has huge potential to further improve the  
396 mechanical properties with use of appropriate coupling agents [16].

397 The variation in specific damping capacity (SDC) was applied in this study to monitor the  
398 anisotropic composites' critical applied stress (CAS) for damage initiation during fatigue  
399 loading. Figures 9a and 9b both indicated that the ISP composites retained distinctly higher  
400 ( $p < 0.01$ ) normalised critical load for damage initiation than the LS composites at equivalent  
401  $V_f$ , indicating that the fatigue damage initiation of the composites was postponed by the ISP  
402 technique. This suggested that the improvement of interfacial strength led to higher critical  
403 applied loads (60% - 70% under dry conditions and 20%-30% under wet conditions) for the  
404 on-set of progressive composite fatigue damage. Similar behaviour was also reported by  
405 Gassan et al. [38] on investigations of tension-tension fatigue of natural fibre reinforced  
406 composites (made by resin transfer moulding), where 10%-30% increase in values of  
407 Critical Applied Load (CAL) for damage initiation were achieved via application of alkaline

408 and saline coupling agents. Flexural fatigue studies conducted on unidirectional (UD) glass  
409 fibre reinforced epoxy composites, revealed that a stronger fibre-matrix interface via  
410 treatment using a commercial saline coupling agent delayed the matrix cracking, thus  
411 increasing the fatigue life of the UD composites by ~20% [55, 56].

412 It was also observed that the LS composites had significantly lower failure strain ( $p < 0.05$ )  
413 than the ISP composites (Equivalent  $V_f$ ), which exhibited that the ISP composites could  
414 sustain increased plastic deformation and damage than their LS counterparts before fatigue  
415 failure (See Figure 7). Similar findings were reported for unidirectional glass fibre  
416 composites, for which failure strain increased with improved fibre/matrix interfacial  
417 properties by applying saline coupling agents [55]. From Figures 7a and 7b, a sudden  
418 increase in the failure strain was observed for both LS and ISP composites, where the  
419 critical stress levels for the onset of the failure strain increase were found to be identical to  
420 the critical loading levels in SDC (60% and 50% of UFS for D-ISP35/50 and D-LS35/50  
421 respectively, 40% for all composites in wet conditions). This relationship between SDC and  
422 failure strain for the PCL/PGF composites provided strong evidence that the critical  
423 stresses for onset of significant fatigue damage observed in this study correlated well and  
424 should be taken into consideration.

#### 425 **4.2. Influence of fluid immersion**

426 It was also observed that the wet testing conditions led to a significant decrease ( $p < 0.0001$ )  
427 in the fatigue life of the PCL/PGF composites, with a 10 and 9-fold reduction observed in LS  
428 and ISP composites respectively (See Figure 6). Deterioration of the fatigue strength in wet  
429 conditions was also noted as the slopes of the SN diagram became significantly steeper  
430 from dry to wet conditions (represented by coefficient 'b', in Table 4). Fluids, such as water  
431 and PBS solution, are able to diffuse into the composites and weaken both the matrix and  
432 the fibre/matrix interface [57]. Our previous study [13] showed that the fibre/matrix interface  
433 plasticisation for both ISP and LS composites occurred readily at 37 °C in PBS.  
434 Degradation of PGFs at or near the PGF fibre/matrix interface within PBS solution can  
435 further influence the fibre/matrix bonding leading to reduction of composite mechanical  
436 properties. Degradation of the fibre/matrix interface is known to increase the damage  
437 accumulation rate under cyclic fatigue loading, hence significantly reducing fatigue life [57,  
438 58]. Similar reductions in fatigue life were also reported by several studies on glass and  
439 carbon fibre reinforced composites and degradation of fibre/matrix interface was stated as  
440 the main cause [57, 59-61]. Liao et al. [59] investigated flexural fatigue on vinyl ester/E-



441 glass composites in water and NaCl solutions at ambient temperature. They observed  
442 significant reductions in fatigue life at low stresses in both media. McBagonluri et al. [60]  
443 also investigated UD pultruded E-glass/vinyl ester composites subjected to flexural  
444 environmental fatigue tests performed in a fluid cell with salt water at 65 °C. They reported  
445 that fatigue life was considerably reduced (~55%) due to fluid immersion. Furthermore, a  
446 flexural fatigue study conducted by Sumsion et al. [62] on UD graphite/epoxy composites in  
447 water and air at ambient temperature, revealed a significant decrease in fatigue life (~47%)  
448 which was suggested to be caused by water attack of the fibre/matrix interface.

449 It was further observed that at high testing stress levels (70% & 80% of UFS), there were  
450 no vast differences in the composites' fatigue life between dry and wet testing conditions  
451 (See Figure 6). A significant difference only began to emerge when the composites were  
452 tested at lower stress levels (30%~60% of UFS). This behaviour suggested that damage  
453 accumulation progressed slower at lower stress levels for LS and ISP composites.  
454 Meanwhile, higher stress levels resulted in stress-dependent fatigue behaviour resulting in  
455 faster damage accumulation. This behaviour was also reported by Liao et al. [59]  
456 investigating fatigue behaviour of E-glass/vinyl ester composites, which showed that the  
457 composites fatigue life was stress-dominated at higher stress levels.

458 It was evident from Figure 8a that, in the dry environment, an initial increase in stiffness at  
459 the early stage of the composites' fatigue life (~5% of  $N_f$ ) had occurred, before the gradual  
460 decline to failure. One possible explanation was due to the presence of voids and void  
461 tunnels inside the composites, which had perhaps closed due to the applied cyclic loading,  
462 making the composites more compact and stiffer. This explanation was supported by the  
463 fact that the LS composites showed a larger increase in stiffness than the ISP composites  
464 (See Figure 8a), and it was previously reported that LS composites generally possessed  
465 higher void content than their ISP counterparts [13]. However, it is very difficult to observe  
466 or measure this behaviour during the fatigue tests, which distinctive proves of the voids  
467 collapsing were not found.

468 Another possible explanation for this observation could be due to reorientation of any  
469 initially off-axis fibre filaments. During the fibre manufacture, the initial fibres collected on  
470 the fibre winding drum were sprayed with PCL solution (Mixed with Chloroform) to maintain  
471 alignment. However, the removal of PCL coated fibre from the drum and the insertion into  
472 the composite manufacturing moulds could have caused some fibres to become miss-

473 aligned. Furthermore, since the phosphate glass fibre mat was bound with PCL prior to  
474 moulding, the high temperature and pressure during LS and ISP composites manufacture  
475 could have induces a level of off-axis fibre filaments, which could have potentially become  
476 unidirectionally reoriented during the fatigue cyclic loading, consequently leading to the  
477 initial increase in stiffness observed. Similar behaviour was observed in natural fibre  
478 reinforced polyester composites, in which the fibrils of the plant fibre reoriented during  
479 tensile fatigue tests and initially increased the composite stiffness [44, 63]. In addition,  
480 Betanzos et. al [15] applied cyclic pressure during the compression moulding stage of PGF  
481 reinforced polylactic acid (PLA) composites, where the composites showed significantly  
482 lower void levels, stronger matrix/fibre interfacial bonding, more uniform fibre alignment and  
483 an increase in flexural modulus. It must be noted that the initial stiffness increase was not  
484 expected and is rarely observed, further investigations into this cause will be required.

485 However, Figure 8b showed that the stiffness increase diminished in wet conditions,  
486 replaced by a significant decrease in stiffness from the beginning of the fatigue tests. The  
487 same change in stiffness variation was also observed when composites were tested at  
488 higher stress levels ( $> 50\%$  UFS) in dry conditions. Both variations can be explained by the  
489 earlier onset and faster progress of fatigue damage caused by media attack and increased  
490 testing stresses. With the fibre/matrix de-bonding and/or fibre fractures occurring inside the  
491 composites, the effects of voids and void channels closing and/or fibre filament  
492 reorientation were insignificant. Moreover, fibre/matrix interface failure occurs readily near  
493 the void sites, which could considerably reduce the chances of voids closing due to cyclic  
494 loading [64, 65].

495 The wet environment also had a clear effect on the PCL/PGF composites' fatigue failure  
496 modes. Figure 11 showed that the dominant failure mode in the dry condition was  
497 compressive delamination and interlaminar shear fracture for the LS composites, whilst ISP  
498 composites showed a clean centre fracture. Immersion in PBS at  $37\text{ }^{\circ}\text{C}$  led to a distinctly  
499 more ductile behaviour (composite softening) for ISP and LS composites, which resulted  
500 from significant weakening of the fibre matrix interfaces. Figure 11f even showed the fibres  
501 sliding out sideways as the loading cycles continued, indicating loss of the fibre/matrix  
502 interface had occurred. Comparing Figures 7a and 7b, the overall strain to failure was  
503 significantly increased ( $p < 0.01$ ) by the introduction of PBS for both ISP and LS composites,  
504 which correlated well with the change from brittle to more ductile dominated failure mode.  
505 This suggested that considerably more plastic deformation and fatigue damage had

506 occurred in wet conditions. The immersion in PBS solution also led to lower critical applied  
507 load (See Table 5), which indicated that earlier onset of progressive fatigue damage had  
508 occurred for the wet composites.

### 509 **4.3. Influence of fibre content**

510 It is well known that the mechanical properties of fibre reinforced composites can be  
511 adjusted by varying their fibre volume fraction ( $V_f$ ). The behaviour of fibre reinforced  
512 composites under cyclic loading is also significantly affected by fibre content [66, 67]. In dry  
513 conditions, the quasi-static data in Table 3 showed that the UFS increased with increasing  
514  $V_f$  for both LS and ISP composites. Meanwhile, in wet conditions, the UFS decreased with  
515 increasing  $V_f$  for both LS and ISP composites. As mentioned earlier, the reduction in UFS  
516 was mainly caused by plasticisation due to PBS ingress along the fibres disrupting the fibre  
517 matrix interface, which severely reduced interfacial strength, and hence the reduction in  
518 UFS was seen. With increasing fibre content, there was much greater fibre/matrix interfacial  
519 area, hence the reduction of UFS was found to be more substantial in the higher volume  
520 fraction composites.

521 Regardless of the testing conditions, it can be seen from Figures 6a and 6b that the  
522 composites' fatigue life decreased significantly ( $p < 0.01$ ) with increasing fibre content for  
523 both LS and ISP composites. Many studies have reported that composite fatigue resistance  
524 had a tendency to deteriorate with increasing fibre volume fraction [68-70]. There are three  
525 main reasons responsible for this reduction: (i) increased fibre-fibre interactions, (ii)  
526 increased fibre/matrix interfaces and (iii) increased regions with high local  $V_f$  resulting from  
527 increased fibre bundle compaction. Although it is widely recognized that enhancement of  
528 composite mechanical properties result from effective stress transfer through fibre/matrix  
529 interfaces, it must also be noted that the fibre/matrix interface is also the region subject to  
530 the largest stress/strain variation [31]. Thus, micro-cracks mostly tend to initiate and grow  
531 from the interfaces [31]. Comparing Figures 10a and 10c to 10b and 10d, it was evident that  
532 PGFs were significantly more compacted with much more fibres close to or touching each  
533 other in the 50%  $V_f$  composites than in the 35%  $V_f$  composites. This resulted in higher  
534 stress/strain gradients at the interface and hence accelerated crack propagation, reducing  
535 fatigue life.

536 In dry conditions, both LS and ISP composites demonstrated a higher critical loading value  
537 for damage initiation with increasing fibre content (See Table 5). However, in wet conditions,

538 a lower critical loading value was noted with increasing fibre content for both of the LS and  
539 ISP composites (See Table 5). This suggested that increasing fibre content could lead to  
540 lower stress thresholds for onset of composite fatigue failure in wet conditions. On the other  
541 hand, no significant difference ( $p>0.05$ ) was found in the degradation rate of composites  
542 fatigue strength (b coefficient) between 35% and 50%  $V_f$  composites when the same  
543 manufacturing technique was applied (see Table 4). This indicated that the degradation rate  
544 of fatigue strength could be independent on fibre content for PCL/PGF LS and ISP  
545 composites. This behaviour also suggested that increasing fibre content didn't have a  
546 significant effect on the rate of fatigue damage accumulation. Similar behaviour of  
547 composites was also described by Shah et al. [71] where no significant variation in  
548 degradation rate of fatigue strength was noted due to varying fibre content for natural fibre  
549 composites.

550 This paper reports for the first time the cyclic fatigue behaviour of fully bioresorbable  
551 PCL/PGF composites. Studies demonstrated that ISP composites had a significantly longer  
552 flexural fatigue life ( $p<0.0001$ ) and superior fatigue damage resistance in comparison to  
553 their LS counterparts. The presence of media (PBS in this case) substantially reduced the  
554 performance of the PCL/PGF composites in both fatigue life and damage resistance.  
555 Increasing fibre content (from 35% to 50%) also resulted in reduced fatigue life, but no  
556 significant difference was observed for the degradation of composite fatigue strength and  
557 damage accumulation behaviours. Amongst all the composites investigated, the ISP35  
558 samples showed a minimum fatigue life of  $10^5$  and  $10^6$  cycles up to 50% test stress levels in  
559 dry and wet conditions respectively (See Figure 6). The ISP35 also maintained at least 50%  
560 of its initial stiffness and strength ( $\sim 6.5$  GPa;  $\sim 85$  MPa) at the end of the fatigue tests in  
561 both dry and wet conditions (See Figure 8), which was comparable to the flexural properties  
562 of human cortical bone (5 – 23 GPa; 35-280 MPa) [53]. Therefore, it can be advised that  
563 the fatigue life and the degradation profile of fatigue strength observed for ISP35  
564 composites were well matched with human cortical bones, suggesting their potential  
565 suitability for bone fracture fixation applications.

## 566 **5. Conclusions**

567 Wet and dry fatigue behaviour of PCL/PGF composites (ISP and LS) was investigated in  
568 this paper. Significantly longer flexural fatigue life ( $p<0.0001$ ) and superior fatigue damage  
569 resistance were observed for ISP composites than LS composites in both dry and wet

570 conditions, which indicated that the ISP process promoted considerably stronger interfacial  
571 bonding than the LS processes. Immersion in PBS during the flexural fatigue tests resulted  
572 in significant reduction ( $p < 0.0001$ ) of the composites fatigue life, earlier onset of fatigue  
573 damage and faster damage propagation. This was attributed to interface plasticisation  
574 (fibre/matrix) caused by PBS diffusion, which resulted in severely weakened interfacial  
575 strength, thus adversely affecting both the quasi-static and fatigue performances of the  
576 PCL/PGF composites. Regardless of testing conditions, increasing fibre content (from 35%  
577 to 50%) resulted in shorter fatigue life for the PCL/PGF composites. However, the  
578 degradation rate of fatigue strength and damage accumulation rate were not significantly  
579 affected by increasing fibre content. Interlaminar shear fracture and clean centre fracture  
580 were observed as the dominant failure modes for LS and ISP composites respectively in  
581 the dry condition. Meanwhile, media immersion resulted in both LS and ISP composites  
582 being softened during the fatigue tests, which led to a more ductile failure mode.

583 In conclusion, this paper demonstrated for the first time the flexural cyclic fatigue behaviour  
584 of fully bioresorbable ISP and LS PCL/PGF composites. ISP35 maintained at least 50% of  
585 its flexural strength and modulus after the fatigue tests, which was well within the range of  
586 the mechanical properties of the human cortical bones.

### 587 **Acknowledgements**

588 The author would like to acknowledge the University of Nottingham for awarding this  
589 studentship through the Dean of Engineering Research Scholarship for International  
590 Excellence. This research did not receive any specific grant from funding agencies in the  
591 public, commercial, or not-for-profit sectors.

### 592 **References**

- 593 [1] Langer R. Tissue Engineering: A New Field and Its Challenges. *Pharm Res*  
594 1997;14:840-1.
- 595 [2] Hubbell JA. Biomaterials in Tissue engineering. Nature Publishing Company  
596 1995;13:565-76.
- 597 [3] Ahmed I, Cronin PS, Abou Neel EA, Parsons AJ, Knowles JC, Rudd CD. Retention of  
598 mechanical properties and cytocompatibility of a phosphate-based glass fiber/poly(lactic  
599 acid) composite. *Journal of Biomedical Materials Research Part B: Applied Biomaterials*  
600 2009;89B:18-27.
- 601 [4] Ahmed I, Parsons AJ, Palmer G, Knowles JC, Walker GS, Rudd CD. Weight loss, ion  
602 release and initial mechanical properties of a binary calcium phosphate glass fibre/PCL  
603 composite. *Acta biomaterialia* 2008;4:1307-14.

- 604 [5] Felfel RM, Ahmed I, Parsons AJ, Walker GS, Rudd CD. In vitro degradation, flexural,  
605 compressive and shear properties of fully bioresorbable composite rods. *Journal of the*  
606 *Mechanical Behavior of Biomedical Materials* 2011;4:1462-72.
- 607 [6] Parsons A, Ahmed I, Niazi M, Habeb R, Fitzpatrick B, Walker G, et al. Mechanical and  
608 degradation properties of phosphate based glass fibre/PLA composites with different fibre  
609 treatment regimes. *Science and Engineering of Composite Materials* 2010;17:243-60.
- 610 [7] Brauer D, Rüssel C, Vogt S, Weisser J, Schnabelrauch M. Degradable phosphate glass  
611 fiber reinforced polymer matrices: mechanical properties and cell response. *J Mater Sci:*  
612 *Mater Med* 2008;19:121-7.
- 613 [8] Knowles JC. Phosphate based glasses for biomedical applications. *Journal of Materials*  
614 *Chemistry* 2003;13:2395-401.
- 615 [9] Lehtonen TJ, Tuominen JU, Hiekkanen E. Dissolution behavior of high strength  
616 bioresorbable glass fibers manufactured by continuous fiber drawing. *Journal of the*  
617 *Mechanical Behavior of Biomedical Materials* 2013;20:376-86.
- 618 [10] Parsons AJ, Ahmed I, Haque P, Fitzpatrick B, Niazi MIK, Walker GS, et al. Phosphate  
619 Glass Fibre Composites for Bone Repair. *Journal of Bionic Engineering* 2009;6:318-23.
- 620 [11] Mohammadi MS, Ahmed I, Muja N, Rudd CD, Bureau MN, Nazhat SN. Effect of  
621 phosphate-based glass fibre surface properties on thermally produced poly(lactic acid)  
622 matrix composites. *Journal of materials science Materials in medicine* 2011;22:2659-72.
- 623 [12] Ahmed I, Collins CA, Lewis MP, Olsen I, Knowles JC. Processing, characterisation and  
624 biocompatibility of iron-phosphate glass fibres for tissue engineering. *Biomaterials*  
625 2004;25:3223-32.
- 626 [13] Chen M, Parsons AJ, Felfel RM, Rudd CD, Irvine DJ, Ahmed I. In-situ polymerisation of  
627 fully bioresorbable polycaprolactone/phosphate glass fibre composites: In vitro degradation  
628 and mechanical properties. *Journal of the mechanical behavior of biomedical materials*  
629 2016;59:78-89.
- 630 [14] Hasan M, Ahmed I, Parsons A, Walker G, Scotchford C. Cytocompatibility and  
631 Mechanical Properties of Short Phosphate Glass Fibre Reinforced Polylactic Acid (PLA)  
632 Composites: Effect of Coupling Agent Mediated Interface. *Journal of Functional*  
633 *Biomaterials* 2012;3:706-25.
- 634 [15] Barrera Betanzos F, Gimeno-Fabra M, Segal J, Grant D, Ahmed I. Cyclic pressure on  
635 compression-moulded bioresorbable phosphate glass fibre reinforced composites.  
636 *Materials & Design* 2016;100:141-50.
- 637 [16] Jiang G, Evans ME, Jones IA, Rudd CD, Scotchford CA, Walker GS. Preparation of  
638 poly( $\epsilon$ -caprolactone)/continuous bioglass fibre composite using monomer transfer moulding  
639 for bone implant. *Biomaterials* 2005;26:2281-8.
- 640 [17] Corden TJ, Jones IA, Rudd CD, Christian P, Downes S. Initial development into a novel  
641 technique for manufacturing a long fibre thermoplastic bioabsorbable composite: in-situ  
642 polymerisation of poly- $\epsilon$ -caprolactone. *Composites Part A: Applied Science and*  
643 *Manufacturing* 1999;30:737-46.
- 644 [18] Christian P, Jones IA, Rudd CD, Campbell RI, Corden TJ. Monomer transfer moulding  
645 and rapid prototyping methods for fibre reinforced thermoplastics for medical applications.  
646 *Composites Part A: Applied Science and Manufacturing* 2001;32:969-76.
- 647 [19] Corden TJ, Jones IA, Rudd CD, Christian P, Downes S, McDougall KE. Physical and  
648 biocompatibility properties of poly- $\epsilon$ -caprolactone produced using in situ polymerisation: a  
649 novel manufacturing technique for long-fibre composite materials. *Biomaterials*  
650 2000;21:713-24.
- 651 [20] McKibbin B. The biology of fracture healing in long bones. *J Bone Joint Surg [Br:*  
652 *Citeseer*; 1978.

- 653 [21] Giannoudis PV, Einhorn TA, Marsh D. Fracture healing: The diamond concept. *Injury*  
654 2007;38:S3-S6.
- 655 [22] An YH, Woolf SK, Friedman RJ. Pre-clinical in vivo evaluation of orthopaedic  
656 bioabsorbable devices. *Biomaterials* 2000;21:2635-52.
- 657 [23] Frost H. The biology of fracture healing: an overview for clinicians. Part I. Clinical  
658 orthopaedics and related research 1989;248:283-93.
- 659 [24] Liao K, Schultheisz CR, Hunston DL, Brinson LC. Long-term durability of fiber-  
660 reinforced polymer-matrix composite materials for infrastructure applications: a review.  
661 *Journal of advanced materials* 1998;30:3-40.
- 662 [25] Vauthier E, Abry J, Bailliez T, Chateauminois A. Interactions between hygrothermal  
663 ageing and fatigue damage in unidirectional glass/epoxy composites. *Composites Science*  
664 *and Technology* 1998;58:687-92.
- 665 [26] Jones C, Dickson R, Adam T, Reiter H, Harris B. The environmental fatigue behaviour  
666 of reinforced plastics. *Proceedings of the Royal Society of London A: Mathematical,*  
667 *Physical and Engineering Sciences: The Royal Society;* 1984. p. 315-38.
- 668 [27] Malpot A, Touchard F, Bergamo S. Influence of moisture on the fatigue behaviour of a  
669 woven thermoplastic composite used for automotive application. *Materials & Design*  
670 2016;98:12-9.
- 671 [28] Stinchcomb W, Reifsnider K. Fatigue damage mechanisms in composite materials: a  
672 review. *Fatigue mechanisms: ASTM International;* 1979.
- 673 [29] Sakin R, Ay İ, Yaman R. An investigation of bending fatigue behavior for glass-fiber  
674 reinforced polyester composite materials. *Materials & Design* 2008;29:212-7.
- 675 [30] Liang S, Gning PB, Guillaumat L. A comparative study of fatigue behaviour of  
676 flax/epoxy and glass/epoxy composites. *Composites Science and Technology* 2012;72:535-  
677 43.
- 678 [31] Vassilopoulos AP, Keller T. *Fatigue of fiber-reinforced composites: Springer Science &*  
679 *Business Media;* 2011.
- 680 [32] Caprino G, D'Amore A. Flexural fatigue behaviour of random continuous-fibre-  
681 reinforced thermoplastic composites. *Composites Science and Technology* 1998;58:957-65.
- 682 [33] Cox BN, Marshall DB. CRACK BRIDGING IN THE FATIGUE OF FIBROUS  
683 COMPOSITES. *Fatigue & Fracture of Engineering Materials & Structures* 1991;14:847-61.
- 684 [34] Hamad WY. On the mechanisms of cumulative damage and fracture in native cellulose  
685 fibres. *Journal of Materials Science Letters* 1998;17:433-6.
- 686 [35] Aghazadeh Mohandesi J, Majidi B. Fatigue damage accumulation in carbon/epoxy  
687 laminated composites. *Materials & Design* 2009;30:1950-6.
- 688 [36] Shiri S, Yazdani M, Pourgol-Mohammad M. A fatigue damage accumulation model  
689 based on stiffness degradation of composite materials. *Materials & Design* 2015;88:1290-5.
- 690 [37] Hwang SJ, Gibson RF, Singh J. Decomposition of coupling effects on damping of  
691 laminated composites under flexural vibration. *Composites Science and Technology*  
692 1992;43:159-69.
- 693 [38] Gassan J. A study of fibre and interface parameters affecting the fatigue behaviour of  
694 natural fibre composites. *Composites Part A: Applied Science and Manufacturing*  
695 2002;33:369-74.
- 696 [39] Lu J, Sun W, Becker A, Saad AA. Simulation of the fatigue behaviour of a power plant  
697 steel with a damage variable. *International Journal of Mechanical Sciences* 2015;100:145-  
698 57.
- 699 [40] Mao H, Mahadevan S. Fatigue damage modelling of composite materials. *Composite*  
700 *Structures* 2002;58:405-10.
- 701 [41] Wu F, Yao W. A fatigue damage model of composite materials. *International Journal of*  
702 *Fatigue* 2010;32:134-8.

- 703 [42] Gamstedt EK, Berglund LA, Peijs T. Fatigue mechanisms in unidirectional glass-fibre-  
704 reinforced polypropylene. *Composites Science and Technology* 1999;59:759-68.
- 705 [43] Lu J, Sun W, Becker A. Material characterisation and finite element modelling of cyclic  
706 plasticity behaviour for 304 stainless steel using a crystal plasticity model. *International*  
707 *Journal of Mechanical Sciences* 2016;105:315-29.
- 708 [44] Shah DU. Damage in biocomposites: Stiffness evolution of aligned plant fibre  
709 composites during monotonic and cyclic fatigue loading. *Composites Part A: Applied*  
710 *Science and Manufacturing* 2016;83:160-8.
- 711 [45] *The Mechanical Properties of Cortical Bone* 1974.
- 712 [46] Bian D, Zhou W, Liu Y, Li N, Zheng Y, Sun Z. Fatigue behaviors of HP-Mg, Mg-Ca and  
713 Mg-Zn-Ca biodegradable metals in air and simulated body fluid. *Acta biomaterialia*  
714 2016;41:351-60.
- 715 [47] van den Oever M, Peijs T. Continuous-glass-fibre-reinforced polypropylene composites  
716 II. Influence of maleic-anhydride modified polypropylene on fatigue behaviour. *Composites*  
717 *Part A: Applied Science and Manufacturing* 1998;29:227-39.
- 718 [48] Reifsnider KL, Schulte K, Duke JC. Long-term fatigue behavior of composite materials.  
719 *Long-term behavior of composites: ASTM International; 1983.*
- 720 [49] Adams RD, Bacon DGC. Measurement of the flexural damping capacity and dynamic  
721 Young's modulus of metals and reinforced plastics. *Journal of Physics D: Applied Physics*  
722 1973;6:27.
- 723 [50] Felfel R, Hossain KZ, Parsons A, Rudd C, Ahmed I. Accelerated in vitro degradation  
724 properties of polylactic acid/phosphate glass fibre composites. *Journal of Materials Science*  
725 2015;50:3942-55.
- 726 [51] Ramakrishnan V, Jayaraman N. Mechanistically based fatigue-damage evolution  
727 model for brittle matrix fibre-reinforced composites. *Journal of Materials Science*  
728 1993;28:5592-602.
- 729 [52] Keusch S, Queck H, Gliesche K. Influence of glass fibre/epoxy resin interface on static  
730 mechanical properties of unidirectional composites and on fatigue performance of cross ply  
731 composites. *Composites Part A: Applied Science and Manufacturing* 1998;29:701-5.
- 732 [53] Bao G, Song Y. Crack bridging models for fiber composites with slip-dependent  
733 interfaces. *Journal of the Mechanics and Physics of Solids* 1993;41:1425-44.
- 734 [54] Subramanian S, Elmore JS, Stinchcomb WW, Reifsnider KL. Influence of fiber-matrix  
735 interphase on the long-term behavior of graphite/epoxy composites. *Composite Materials:*  
736 *Testing and Design: Twelfth Volume: ASTM International; 1996.*
- 737 [55] Shih GC, Ebert LJ. The effect of the fiber/matrix interface on the flexural fatigue  
738 performance of unidirectional fiberglass composites. *Composites Science and Technology*  
739 1987;28:137-61.
- 740 [56] Bledzki A, Wacker G, Frenzel H. Effect of surface-treated glass fibres on the dynamic  
741 behavior of fibre-reinforced composites. *Mechanics of composite materials* 1994;29:429-33.
- 742 [57] Kotsikos G, Evans JT, Gibson AG, Hale JM. Environmentally enhanced fatigue  
743 damage in glass fibre reinforced composites characterised by acoustic emission.  
744 *Composites Part A: Applied Science and Manufacturing* 2000;31:969-77.
- 745 [58] Houghton W, Shuford R, Mitchel J, Sobczak J. NDE of composite rotor blades during  
746 fatigue testing. *Proceedings of the Helicopter Society of America Conference, St*  
747 *Louis* 1980.
- 748 [59] Liao K, Schultheisz CR, Hunston DL. Long-term environmental fatigue of pultruded  
749 glass-fiber-reinforced composites under flexural loading. *International journal of fatigue*  
750 1999;21:485-95.



- 751 [60] McBagonluri F, Garcia K, Hayes M, Verghese K, Lesko J. Characterization of fatigue  
752 and combined environment on durability performance of glass/vinyl ester composite for  
753 infrastructure applications. *International journal of fatigue* 2000;22:53-64.
- 754 [61] Shan Y, Liao K. Environmental fatigue behavior and life prediction of unidirectional  
755 glass-carbon/epoxy hybrid composites. *International Journal of Fatigue* 2002;24:847-59.
- 756 [62] Sumsion H, Williams D. Effects of environment on the fatigue of graphite-epoxy  
757 composites. *Fatigue of composite materials: ASTM International*; 1975.
- 758 [63] Shah DU. Developing plant fibre composites for structural applications by optimising  
759 composite parameters: a critical review. *Journal of Materials Science* 2013;48:6083-107.
- 760 [64] Chambers AR, Earl JS, Squires CA, Suhot MA. The effect of voids on the flexural  
761 fatigue performance of unidirectional carbon fibre composites developed for wind turbine  
762 applications. *International Journal of Fatigue* 2006;28:1389-98.
- 763 [65] Thomason JL. The interface region in glass fibre-reinforced epoxy resin composites: 2.  
764 Water absorption, voids and the interface. *Composites* 1995;26:477-85.
- 765 [66] Chandra R, Singh S, Gupta K. Damping studies in fiber-reinforced composites—a  
766 review. *Composite structures* 1999;46:41-51.
- 767 [67] Saravanos DA, Chamis CC. Unified micromechanics of damping for unidirectional and  
768 off-axis fiber composites. *Journal of Composites, Technology and Research* 1990;12:31-40.
- 769 [68] Mandell JF, Reed RM, Samborsky DD. Fatigue of fiberglass wind turbine blade  
770 materials.
- 771 [69] Samborsky DD. Fatigue of E-glass fiber reinforced composite materials and  
772 substructures: Citeseer; 1999.
- 773 [70] Boller KH. Effect of tensile mean stresses on fatigue properties of plastic laminates  
774 reinforced with unwoven glass fibers. DTIC Document; 1964.
- 775 [71] Shah DU, Schubel PJ, Clifford MJ, Licence P. Fatigue life evaluation of aligned plant  
776 fibre composites through S-N curves and constant-life diagrams. *Composites Science and  
777 Technology* 2013;74:139-49.

778

**Table 1:** Phosphate glass code and formulation

Glass code	P <sub>2</sub> O <sub>5</sub> content (mol%)	CaO content (mol%)	Na <sub>2</sub> O content (mol%)	MgO content (mol%)	Fe <sub>2</sub> O <sub>3</sub> content (mol%)	Drying temp/time (°C/h)	Melting temp/time (°C/h)
P45Fe5	45	16	10	24	5	350/0.5	1100/1.5

**Table 2:** PCL/PGF composites codes (DW refers to dry or wet testing conditions)

Manufacture technique	Composites codes	Fibre Orientation
Laminate Stacking (LS)	(D/W)-LS35	Unidirectional (UD)
	(D/W)-LS50	
In-situ Polymerisation (ISP)	(D/W)-ISP35	
	(D/W)-ISP50	

**Table 3.** Quasi-static flexural properties for all composite specimens

Composites Code	Actual V <sub>f</sub> (%)	Ultimate Flexural Strength (UFS) (MPa)	Flexural Stiffness (E <sub>f</sub> ) (GPa)	Composites Code	Actual V <sub>f</sub> (%)	Ultimate Flexural Strength (UFS) (MPa)	Flexural Stiffness (E <sub>f</sub> ) (GPa)
<b>D-LS35</b>	34 ± 1	126 ± 2	9.1 ± 0.7	<b>D-ISP35</b>	36 ± 1	172 ± 3	14.4 ± 0.6
<b>W-LS35</b>	32 ± 1	110 ± 3	6.2 ± 0.3	<b>W-ISP35</b>	35 ± 1	141 ± 2	13.0 ± 0.2
<b>D-LS50</b>	51 ± 1	143 ± 2	12.7 ± 0.4	<b>D-ISP50</b>	49 ± 2	210 ± 3	18.6 ± 0.4
<b>W-LS50</b>	50 ± 1	105 ± 1	6.3 ± 0.3	<b>W-ISP50</b>	50 ± 1	123 ± 1	12.4 ± 0.4

**Table 4.** Values of 'b' from S-N curve fitting for LS and ISP composites

Sample Code	D-LS35	D-LS50	W-LS35	W-LS50	D-ISP35	D-ISP50	W-ISP35	W-ISP50
<b>b</b>	-0.089	-0.071	-0.497	-0.661	-0.101	-0.131	-0.241	-0.244

**Table 5.** Values of Critical Applied Stress (CAS) for LS and ISP composites

Sample Code	D-LS35	D-LS50	D- ISP35	D-ISP50	W-LS35	W-LS50	W- ISP35	W- ISP50
CAS (MPa)	63	71	103	126	44	42	56	49

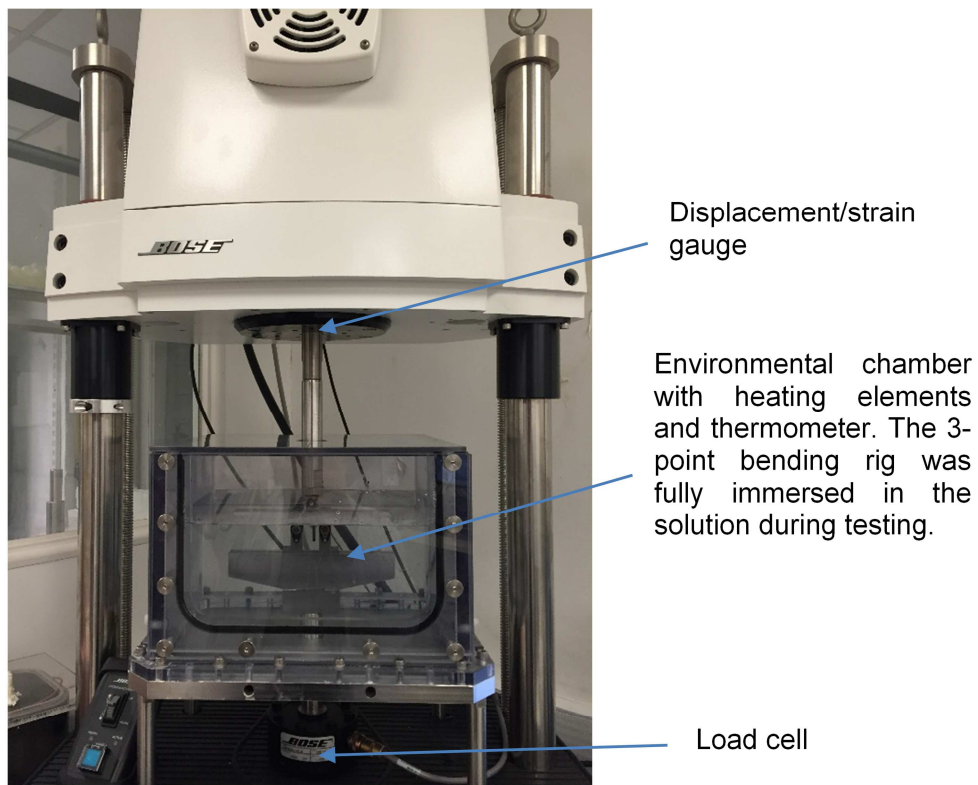


**Figure 1.** Bose ElectroForce® Series II 3330 testing machine equipped with environmental chamber

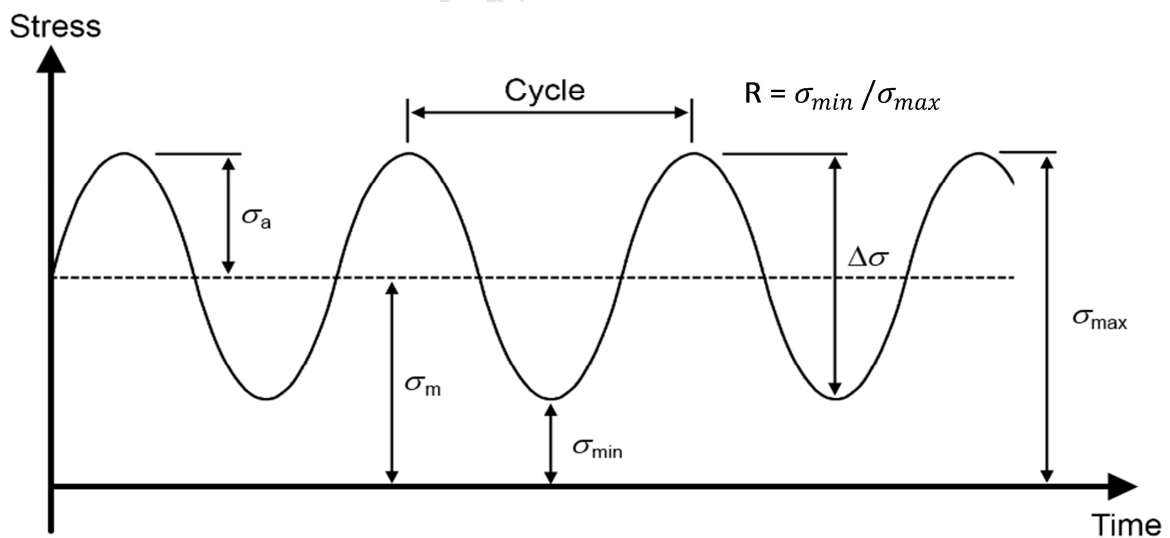


**Figure 2.** Example of sinusoidal constant amplitude load waveforms with term definition and R value

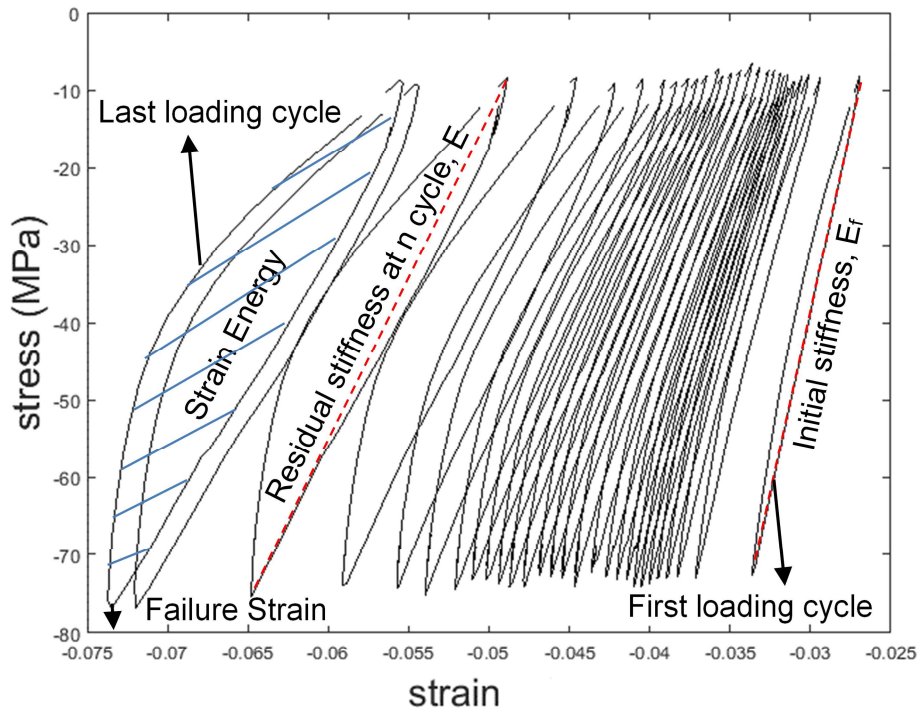


**Figure 3.** Example of stress strain variation during the flexural fatigue tests (the negative sign only indicated the direction as downwards)

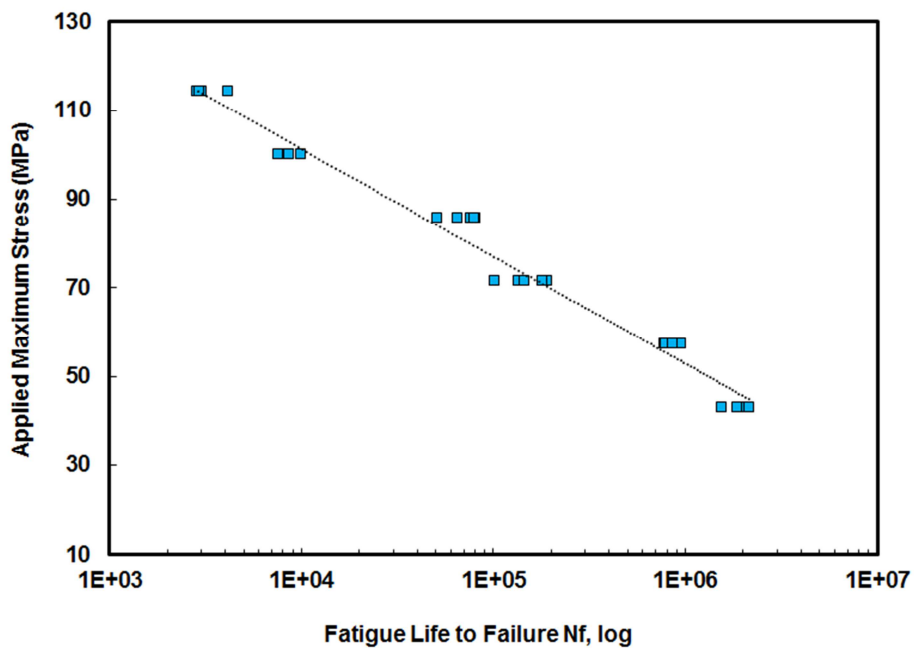


**Figure 4.** Typical S-N diagram with example data

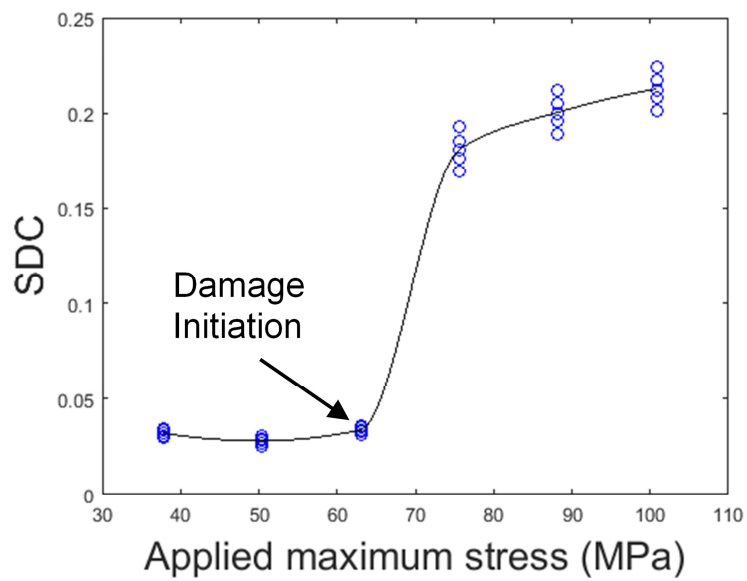


**Figure 5.** Example of Specific Flexural Damping Capacity vs. Applied Maximum Stress for dry LS35 composites

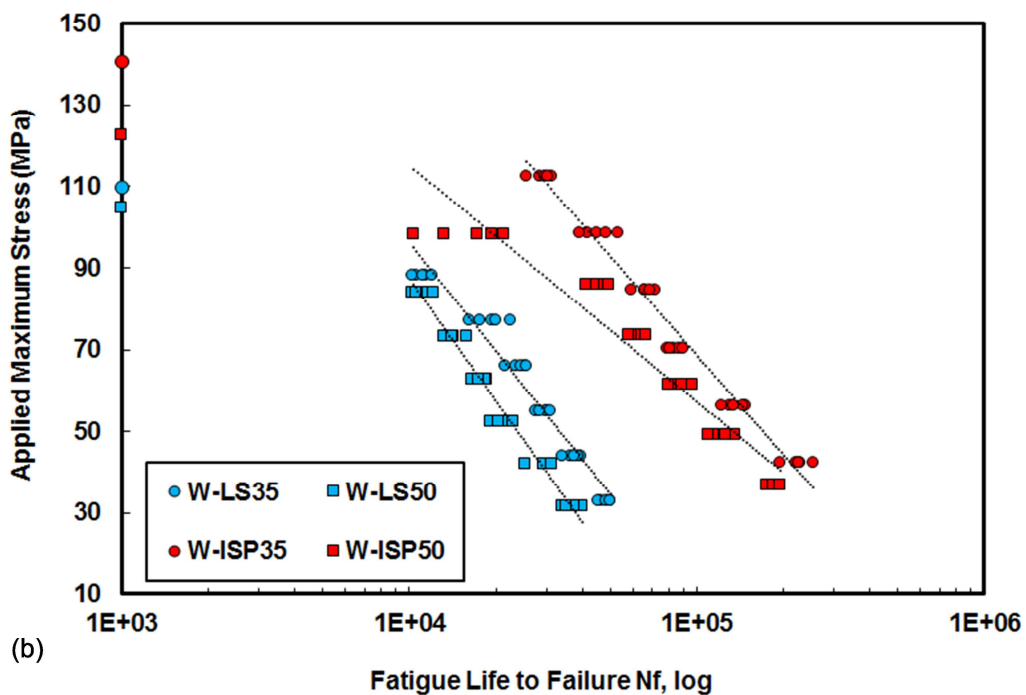
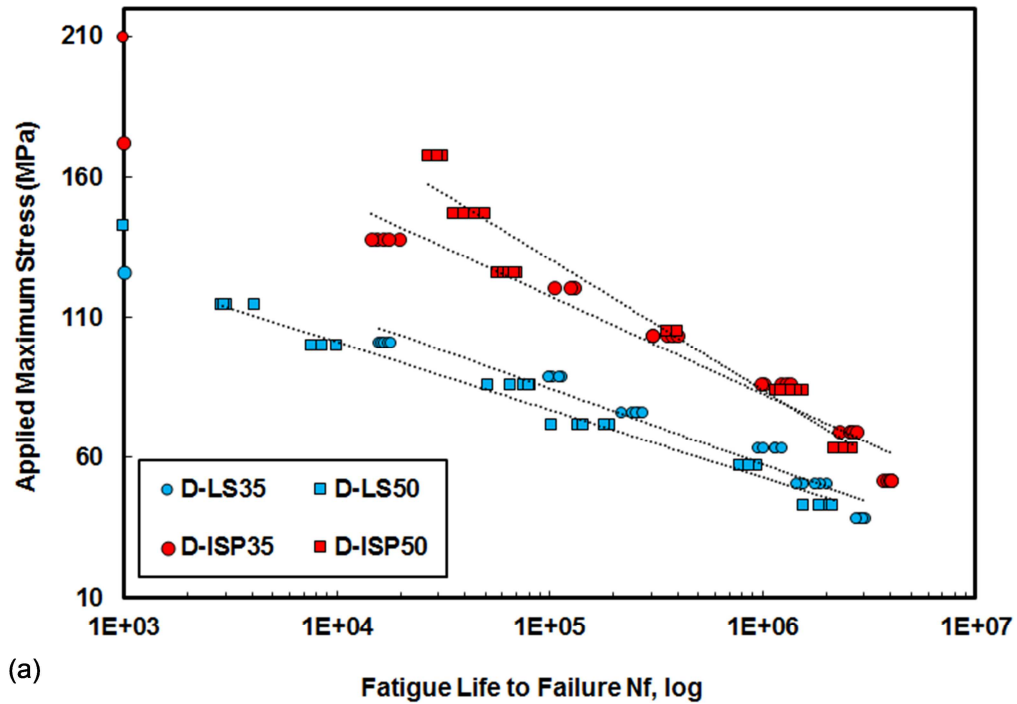


**Figure 6.** S-N diagram of PCL/PGF composites in dry and wet environments plotted in power-law regression scale (points on the y-axis indicate the monotonic flexural strength of the composites): (a) Comparison of composites made by LS and ISP in dry environment; (b) Comparison of composites made by LS and ISP in wet environment. The circles represent 35%  $V_f$  whereas the squared points are representative of 50%  $V_f$  samples.

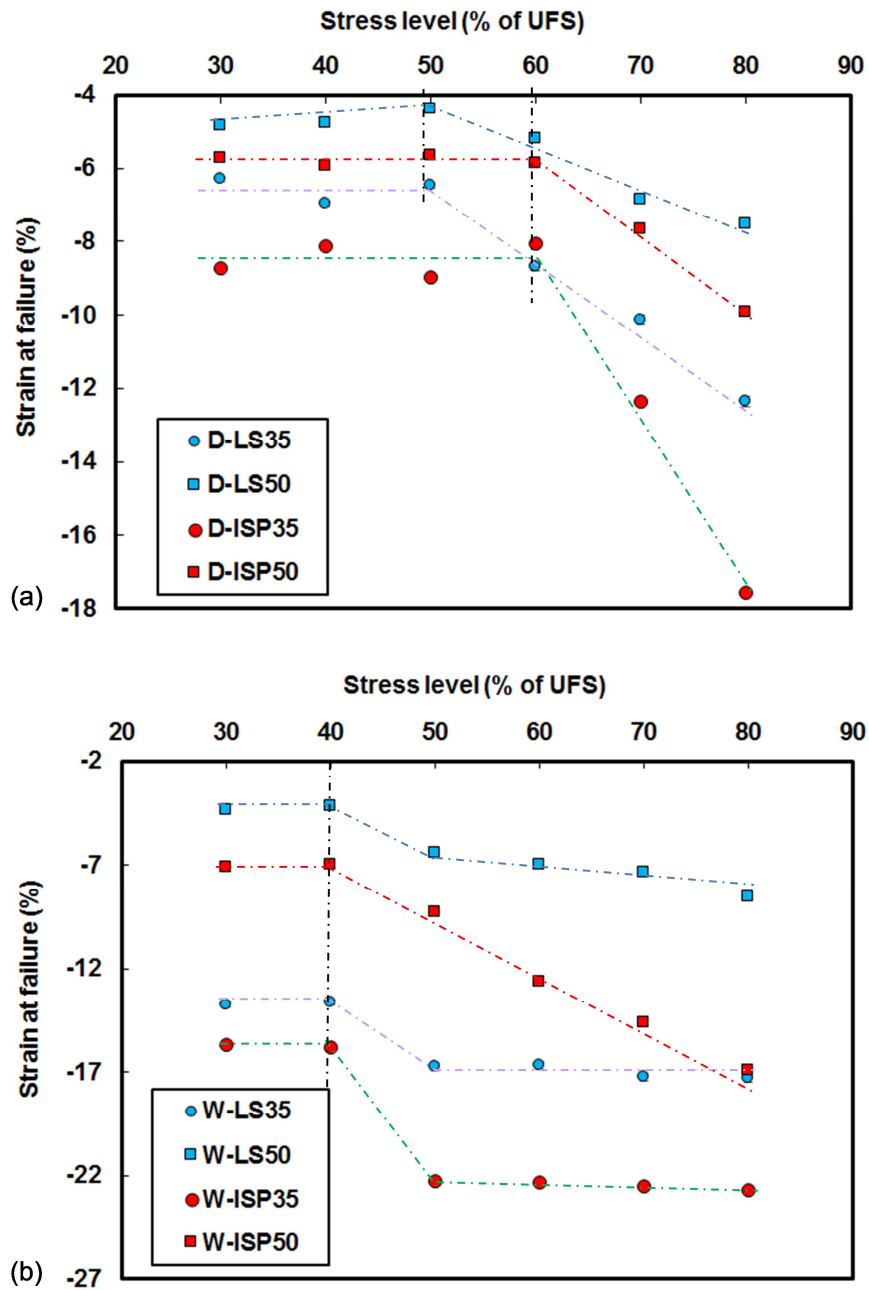


**Figure 7.** Strain at fatigue failure ('-' as downwards) against testing stress levels: (a) LS and ISP composites tested dry; (b) LS and ISP composites tested wet; Error bars fall within the dimension of the markers. Vertical dotted line presents threshold stress level that the failure strains increase significantly, other dotted lines are given as guides to the eyes

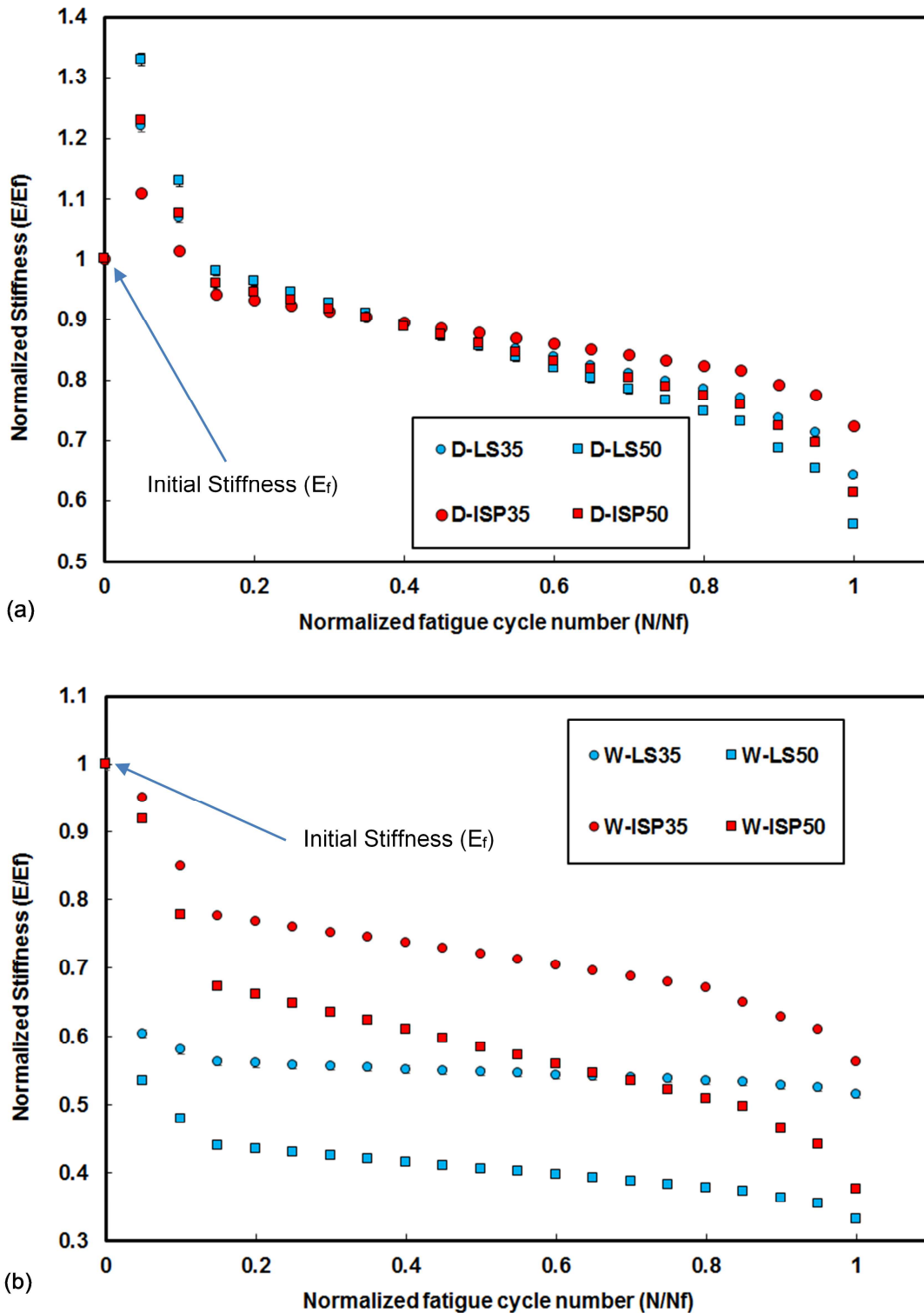


**Figure 8.** Normalised stiffness against normalised cycle number for composites tested at 40% of UFS in: (a) Dry Environment, inset graph for dry composites tested at 60% of UFS; (b) Wet Environment; Error bars fall within the dimension of the markers



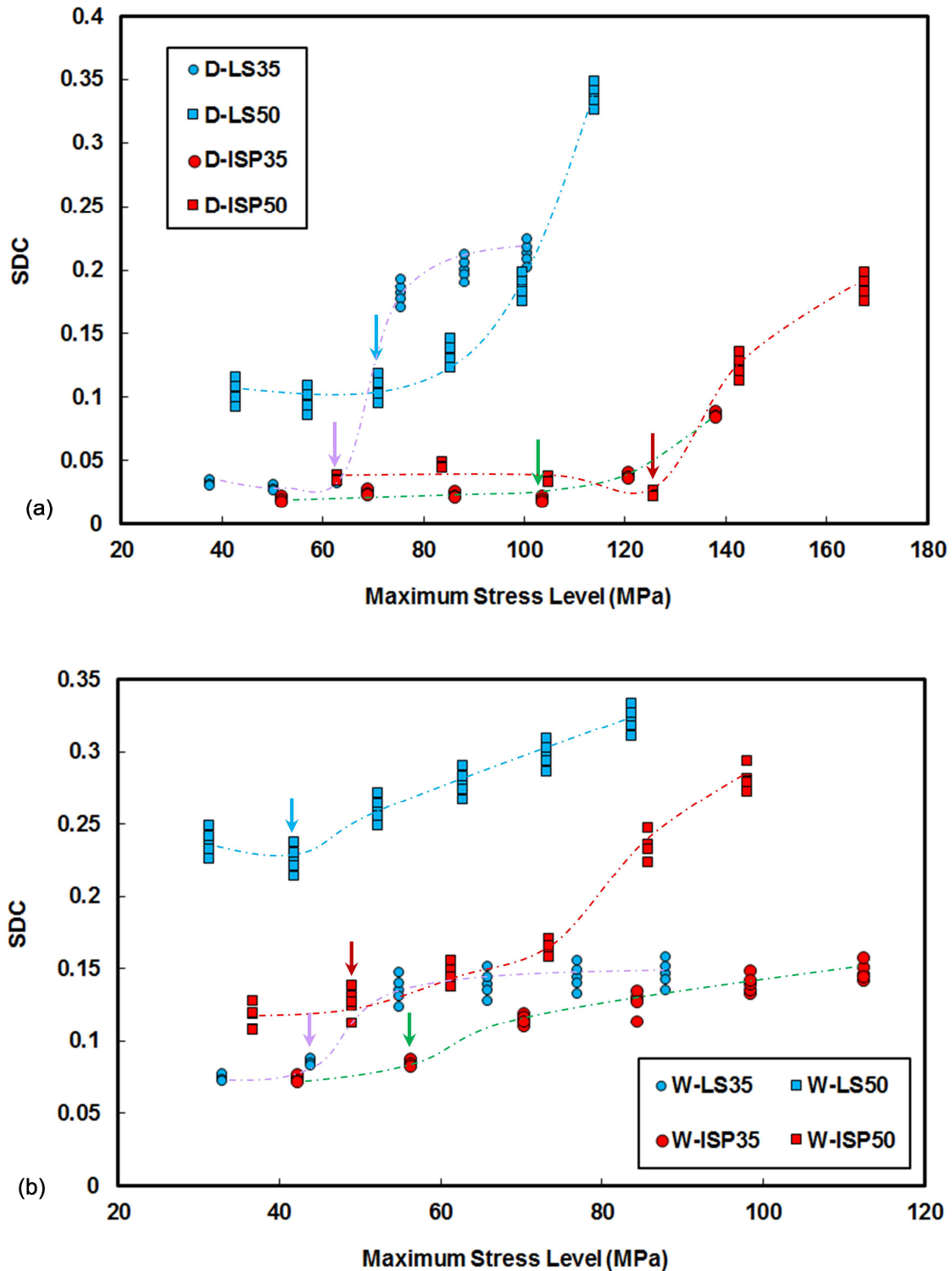
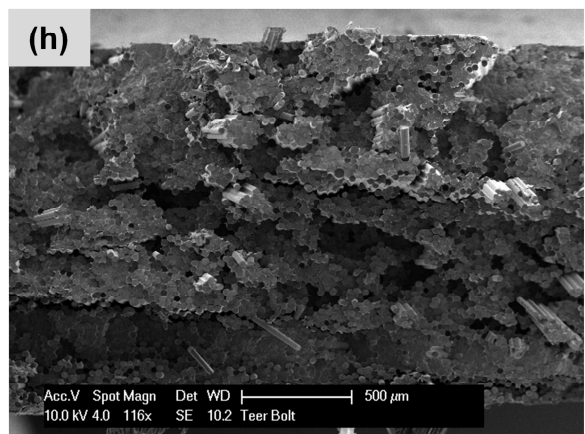
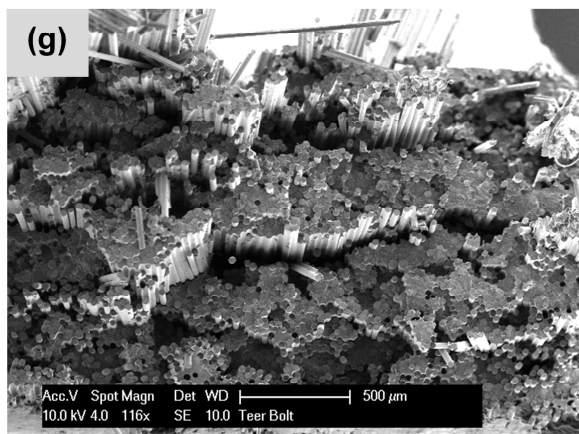
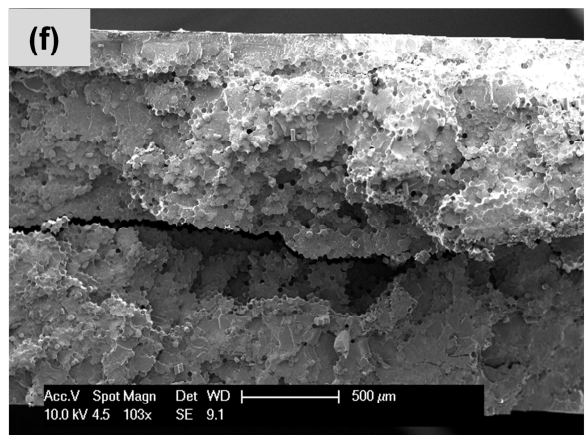
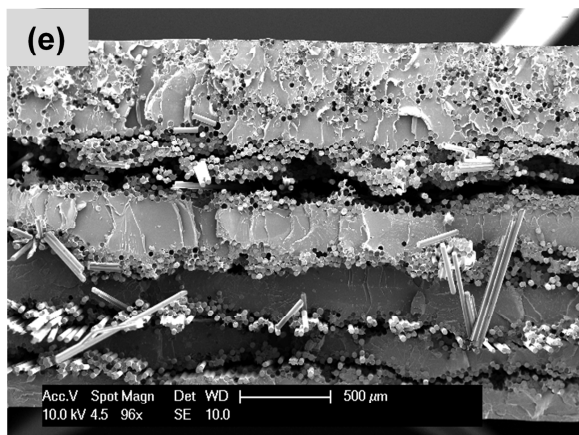
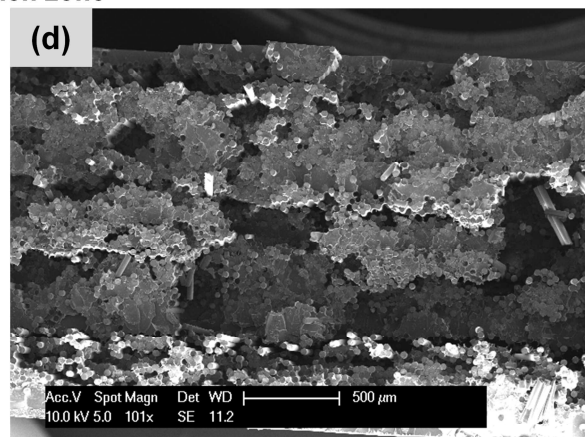
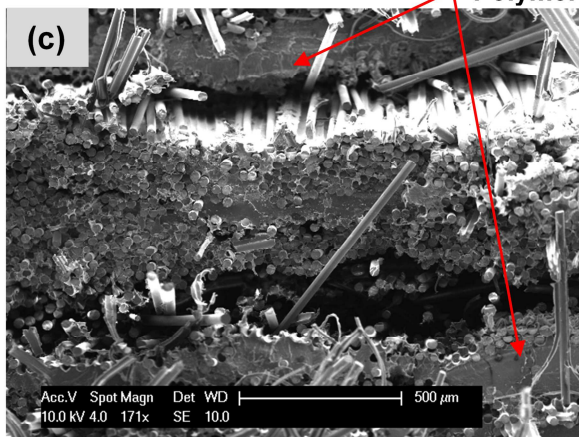
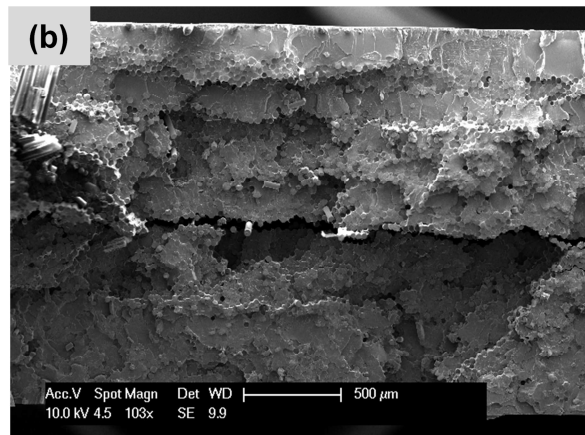
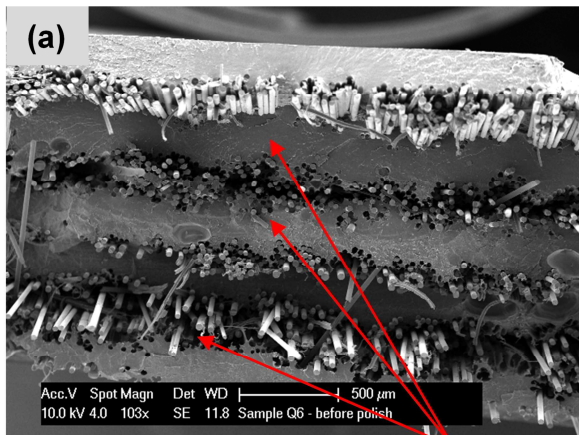


**Figure 9.** Specific flexural damping capacity verses applied maximum load for LS and ISP composites: (a) in dry conditions; (b) in wet conditions; Arrows point to the CAS values of the composites. The dotted lines are given as guides to the eye



Polymer rich zone

**Figure 10.** SEM cross section images of the composites fatigue fracture surfaces: (a) D -LS35; (b) D -ISP35; (c) D -LS50; (d) D -ISP50; (e) W -LS35; (f) W -ISP35; (g) W -LS50; (h) W -ISP50

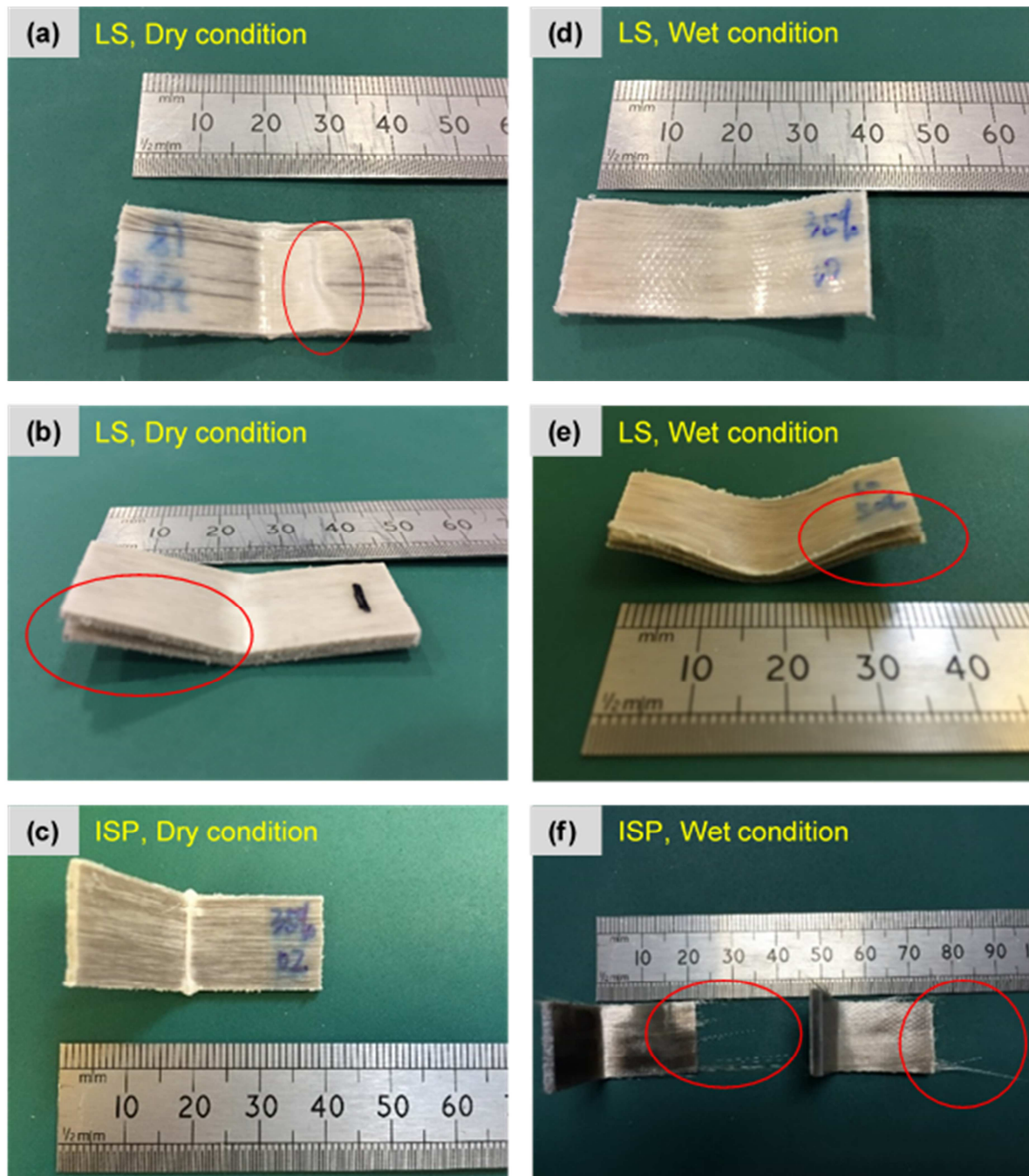


**Figure 11.** Images taken of LS and ISP composites' after end of fatigue testing cycles: (a) compressive delamination was observed (see red circle); (b) interlaminar shear fracture (see red circle); (c) centre fracture where load was applied; (d) softening of sample observed from wet testing; (e) softening and interlaminar shear fracture observed (see red circle); (f) fibre protrusions were also observed post testing (see red circles) and centre fracture were load was applied.